

การสังเคราะห์อนุภาคระดับนาโนเมตรของแพลเลเดียมความเข้มข้นสูง  
โดยใช้ซูโครสที่ถูกปรับปรุงคุณสมบัติเป็นตัวรีดิวซ์

นายลัญจกร อมรกิจบำรุง

วิทยานิพนธ์นี้เป็นส่วนหนึ่งของการศึกษาตามหลักสูตรปริญญาวิทยาศาสตรมหาบัณฑิต  
สาขาวิชาเคมี ภาควิชาเคมี  
คณะวิทยาศาสตร์ จุฬาลงกรณ์มหาวิทยาลัย  
ปีการศึกษา 2554  
ลิขสิทธิ์ของจุฬาลงกรณ์มหาวิทยาลัย

บทคัดย่อและแฟ้มข้อมูลฉบับเต็มของวิทยานิพนธ์ตั้งแต่ปีการศึกษา 2554 ที่ให้บริการในคลังปัญญาจุฬาฯ (CUIR)  
เป็นแฟ้มข้อมูลของนิสิตเจ้าของวิทยานิพนธ์ที่ส่งผ่านทางบัณฑิตวิทยาลัย

The abstract and full text of theses from the academic year 2011 in Chulalongkorn University Intellectual Repository(CUIR)  
are the thesis authors' files submitted through the Graduate School.

SYNTHESIS OF HIGH-CONCENTRATION PALLADIUM NANOPARTICLES  
USING MODIFIED SUCROSE AS REDUCING AGENT

Mr. Lunjakorn Amornkitbamrung

A Thesis Submitted in Partial Fulfillment of the Requirements  
for the Degree of Master of Science Program in Chemistry

Department of Chemistry

Faculty of Science

Chulalongkorn University

Academic Year 2011

Copyright of Chulalongkorn University

Thesis Title           SYNTHESIS OF HIGH-CONCENTRATION PALLADIUM  
                                  NANOPARTICLES USING MODIFIED SUCROSE AS  
                                  REDUCING AGENT

By                         Mr. Lunjakorn Amornkitbamrung

Field of Study         Chemistry

Thesis Advisor        Associate Professor Sanong Ekgasit, Ph.D.

Thesis Co-advisor   Associate Professor Chuchaat Thammacharoen

---

Accepted by the Faculty of Science, Chulalongkorn University in Partial  
Fulfillment of the Requirements for Master's degree

.....Dean of the Faculty of Science  
(Professor Supot Hannongbua, Dr. rer. nat.)

#### THESIS COMMITTEE

.....Chairman  
(Assistant Professor Warinthorn Chavasiri, Ph.D.)

.....Thesis Advisor  
(Associate Professor Sanong Ekgasit, Ph.D.)

.....Thesis Co-advisor  
(Associate Professor Chuchaat Thammacharoen)

.....Examiner  
(Associate Professor Vithaya Ruangpornvisuti, Dr. rer. nat.)

.....External Examiner  
(Assistant Professor Pimthong Thongnopkun, Ph.D.)

ลัญจกร อมรกิจบำรุง : การสังเคราะห์อนุภาคระดับนาโนเมตรของแพลเลเดียมความเข้มข้นสูงโดยใช้ซูโครสที่ถูกรับปรุงคุณสมบัติเป็นตัวรีดิวซ์ (SYNTHESIS OF HIGH-CONCENTRATION PALLADIUM NANOPARTICLES USING MODIFIED SUCROSE AS REDUCING AGENT) อ.ที่ปรึกษาวิทยานิพนธ์หลัก: รศ. ดร.สนอง เอกสิทธิ์, อ.ที่ปรึกษาวิทยานิพนธ์ร่วม: รศ.ชูชาติ ธรรมเจริญ, 53 หน้า.

งานวิจัยนี้ได้พัฒนากรรมวิธีใหม่ที่เป็นมิตรต่อสิ่งแวดล้อมในการสังเคราะห์อนุภาคระดับนาโนเมตรและโครงสร้างระดับไมโครเมตรที่เป็นรูปทรงดอกไม้ของแพลเลเดียมที่มีความเข้มข้นสูง (100-1000 ส่วนในล้านส่วน) โดยใช้ซูโครสซึ่งได้จากผลิตภัณฑ์การเกษตรและไฮโดรเจนเปอร์ออกไซด์เป็นตัวรีดิวซ์ อนุภาคระดับนาโนเมตรที่เป็นทรงกลมและโครงสร้างระดับไมโครเมตรที่เป็นรูปทรงดอกไม้ที่สังเคราะห์ได้มีขนาดของอนุภาคอยู่ในช่วงระหว่าง 100 นาโนเมตร ถึง 5 ไมโครเมตร โดยพบว่าค่าเป็นปัจจัยสำคัญที่ทำให้ซูโครสมีคุณสมบัติเป็นตัวรีดิวซ์ได้ เงื่อนไขและภาวะต่าง ๆ ถูกปรับเปลี่ยนเพื่อสังเคราะห์อนุภาคระดับนาโนเมตรของแพลเลเดียมที่มีขนาดเล็กและมีเสถียรภาพสูง นอกจากนี้ยังสามารถควบคุมขนาดและรูปทรงของโครงสร้างระดับไมโครเมตรที่เป็นรูปทรงดอกไม้ของแพลเลเดียมโดยการเปลี่ยนความเข้มข้นของแพลเลเดียมคลอไรด์และไฮโดรเจนเปอร์ออกไซด์ที่ใช้ในการสังเคราะห์ และจากการทดลองเพื่อศึกษากลไกการเกิดโครงสร้างพบว่า โครงสร้างระดับไมโครเมตรที่เป็นรูปทรงดอกไม้ของแพลเลเดียมเกิดขึ้นจากการจับตัวกันของอนุภาคระดับนาโนเมตรขนาด 3 นาโนเมตร โครงสร้างระดับนาโนเมตรที่เป็นรูปทรงดอกไม้ของแพลเลเดียมมีศักยภาพสูงที่จะถูกนำไปใช้เป็นตัวเร่งปฏิกิริยาที่มีประสิทธิภาพเนื่องจากมีพื้นผิวที่สะอาด

ภาควิชา.....เคมี.....ลายมือชื่อนิสิต.....  
 สาขาวิชา.....เคมี.....ลายมือชื่อ อ. ที่ปรึกษาวิทยานิพนธ์หลัก.....  
 ปีการศึกษา.....2554.....ลายมือชื่อ อ. ที่ปรึกษาวิทยานิพนธ์ร่วม.....

# # 5272514723 : MAJOR CHEMISTRY

KEYWORDS : PALLADIUM / NANOPARTICLES / GREEN CHEMISTRY /  
SUCROSE / HYDROGEN PEROXIDE

LUNJAKORN AMORNKITBAMRUNG : SYNTHESIS OF HIGH-  
CONCENTRATION PALLADIUM NANOPARTICLES USING  
MODIFIED SUCROSE AS REDUCING AGENT. ADVISOR: ASSOC.  
PROF. SANONG EKGASIT, Ph.D., CO-ADVISOR: ASSOC. PROF.  
CHUCHAAT THAMMACHAROEN, 53 pp.

In this work, we have developed a novel green chemistry approach for the synthesis of high-concentration (100-1000 ppm) palladium nanoparticles (PdNPs) and flowerlike palladium microstructures (FPd $\mu$ STs) using reducing agent and stabilizer which are very cheap and harmless to the environment. PdCl $_4^{2-}$  was reduced while the obtained nanoparticles were stabilized by a non-toxic sucrose and hydrogen peroxide (HP). Spherical PdNPs and FPd $\mu$ STs with particle size in the range of 100 nm to 5  $\mu$ m were successfully synthesized. The added sodium hydroxide is a key factor for the generation of reducing species from sucrose. The optimal synthesized condition was determined in order to completely reduce all PdCl $_4^{2-}$  and to produce small PdNPs with high stability. This approach can be scaled-up for the production of high-concentration PdNPs for industrial use with a highly competitive price. Morphology (size and shape) and complexity of the FPd $\mu$ STs could be tuned through the synthetic conditions (i.e., concentrations of PdCl $_4^{2-}$  and HP). The time dependent investigation of FPd $\mu$ STs formation suggested that the FPd $\mu$ STs evolved from PdNPs with a particle size of 3 nm. The naked FPd $\mu$ STs with clean surfaces are expected to possess high catalytic activity.

Department of Study:..... Chemistry..... Student's Signature.....

Field of Study:..... Chemistry..... Advisor's Signature.....

Academic Year:..... 2011..... Co-Advisor's Signature.....

## ACKNOWLEDGEMENTS

I would like to express my sincere gratitude to my thesis advisor, Associate Professor Dr. Sanong Ekgasit and my thesis co-advisor Associate Professor Chuchaat Thammacharoen for wholeheartedly provide the useful guidance, understanding, training and teaching the theoretical background and technical skills during my research.

I would like to thank Assistant Professor Dr. Warinthorn Chavasiri, Associate Professor Dr. Vithaya Ruangpornvisuti, and Assistant Professor Dr. Pimthong Thongnopkun for usefully substantial suggestions as the thesis committee.

Warmest thanks to my friends, my colleagues and organization: Sensor Research Unit, Department of Chemistry, Faculty of Science, Chulalongkorn University, and all good friends for the suggestions and spiritual supports through out this research.

Partial financial support from the National Research Council of Thailand (NRCT), Center of Innovative Nanotechnology Chulalongkorn University (CIN-CU), and National Center of Excellence for Petroleum, Petrochemicals, and Advanced Materials (CE-PPAM).

Whatever shortcomings in the thesis remain, they are the sole responsibility of the author.

Above all, I am profoundly grateful to my parents (Associate Professor Dr. Vittaya Amornkitbamrung and Assistant Professor Sujaree Amornkitbamrung) and endearing family for all their loves, understanding, support, and encouragement during the whole period of my study.

# CONTENTS

	Page
ABSTRACT IN THAI.....	iv
ABSTRACT IN ENGLISH.....	v
ACKNOWLEDGEMENTS.....	vi
CONTENTS.....	vii
LIST OF FIGURES.....	x
LIST OF ABBREVIATIONS.....	xiii
CHAPTER I INTRODUCTION.....	1
1.1 Nanotechnology.....	1
1.2 Nanomaterials and their catalytic usage.....	1
1.3 The research objective.....	3
1.4 The research scopes.....	3
1.5 Benefit of research.....	3
CHAPTER II THEORETICAL BACKGROUND.....	4
2.1 Properties and applications of palladium.....	4
2.2 Synthesis of palladium nanoparticles.....	5
2.3 Synthesis of palladium nanoparticles by chemical reduction.....	8
2.4 Theory on nucleation and growth of metal nanoparticles.....	13
2.5 Stabilization of metal nanoparticles.....	14
CHAPTER III EXPERIMENT.....	16
3.1 Chemicals and materials.....	16
3.2 Synthesis of palladium nanoparticles by using sucrose as a reducing agent.....	16

3.3 Synthesis of palladium nanoparticles by using acidic and alkaline-treated sucrose as reducing agents.....	17
3.3.1 Synthesis of palladium nanoparticles by using acidic-treated sucrose as a reducing agent.....	17
3.3.2 Synthesis of palladium nanoparticles by using alkaline-treated sucrose as a reducing agent.....	17
3.3.3 Synthesis of palladium nanoparticles by using acidic then alkaline-treated sucrose as a reducing agent.....	18
3.4 Preparation of palladium film through self-assembly of palladium nanoparticles at air-water interface.....	18
3.5 Synthesis of flowerlike palladium microstructures by using hydrogen peroxide as a reducing agent.....	19
3.6 Characterization of palladium nanoparticles, palladium film, and flowerlike palladium microstructures.....	19
3.6.1 UV-vis spectroscopy.....	19
3.6.2 Scanning electron microscopy.....	20
3.6.3 Transmission electron microscopy.....	20
3.6.4 Attenuated total reflection Fourier transform infrared spectroscopy.....	20
3.6.5 XRD technique.....	20
CHAPTER IV RESULTS AND DISCUSSION.....	21
4.1 Palladium nanoparticles synthesized by using sucrose as a reducing agent.....	21
4.1.1 Formation of palladium nanoparticles.....	21
4.1.2 UV-vis absorption spectra of palladium nanoparticles.....	22
4.1.3 Morphology of palladium nanoparticles synthesized by using sucrose as a reducing agent .....	25



	Page
4.1.4 TEM images and crystal structure of palladium nanoparticles	29
4.1.5 Degradation of sucrose under acidic condition.....	29
4.1.6 Degradation of monosaccharide under alkaline condition.....	30
4.1.7 Investigation of sucrose degradation under acidic and alkaline conditions by ATR FT-IR spectroscopy.....	34
4.2 Sucrose induced formation of palladium film at air-water interface.....	35
4.2.1 Formation of palladium film at air-water interface.....	35
4.2.2 The time-dependent investigating formation of palladium film at air-water interface .....	36
4.2.3 The crystal structure of palladium film.....	39
4.3 Flowerlike palladium microstructures synthesized by using hydrogen peroxide as a sole reducing agent.....	39
4.3.1 Formation of flowerlike palladium microstructures .....	39
4.3.2 Effect from the concentration of $\text{PdCl}_4^{2-}$ and hydrogen peroxide.....	41
4.3.3 The time-dependent shape evolution of flowerlike palladium microstructures .....	43
4.3.4 The crystal structure of flowerlike palladium microstructures	46
 CHAPTER V CONCLUSIONS.....	 47
 REFERENCES.....	 49
 VITAE.....	 53

## LIST OF FIGURES

Figure	Page
2.1 Applications of palladium catalyst for automobile catalytic converter (A) and hydrogenation reaction (B).....	5
2.2 Applications of palladium catalyst for hydrogen gas fuel cell.....	5
2.3 Schematic illustration of metal nanoparticles preparation by physical and chemical methods .....	7
2.4 Techniques for synthesis of metal nanoparticles by physical method	7
2.5 Synthesis of metal nanoparticles by chemical reduction.....	8
2.6 Cubic shape of PdNPs with the size of 85 nm .....	10
2.7 Cubic, decahedral, octahedral, and rod shapes of PdNPs .....	10
2.8 Flowerlike and polyhedral shapes of PdNPs with the size of 60 to 70 nm .....	12
2.9 Plot of atom concentration and time, showing the nucleation and subsequent growth .....	14
2.10 Schematic illustration of metal nanoparticles stabilized by electrostatic repulsion .....	15
2.11 Schematic illustration of metal nanoparticles stabilized by steric hindrance.....	15
4.1 PdNPs synthesized by using (A) sucrose, (B) alkaline-treated sucrose, (C) acidic-treated sucrose, and (D) acidic then alkaline-treated sucrose as reducing agents .....	22
4.2 UV-vis spectra of (A) PdNPs synthesized by using sucrose treated in various conditions as reducing agents and (B) sucrose treated in various conditions .....	23
4.3 UV-vis spectra of PdNPs synthesized by using (A) sucrose, (B) alkaline-treated, (C) acidic-treated sucrose, and (D) acidic then alkaline-treated sucrose as reducing agents comparing between diluting with NaBH <sub>4</sub> (blue) and DI water (black).....	24

Figure	Page
4.4 SEM micrographs of PdNPs synthesized by using (A) sucrose, (B) alkaline-treated, (C) acidic-treated sucrose, and (D) acidic then alkaline-treated sucrose as reducing agents .....	26
4.5 SEM micrographs of PdNPs synthesized by using acidic then alkaline-treated sucrose as a reducing agent, at (A) lower and (B) higher magnifications, and (C) EDX spectrum.....	27
4.6 (A-C) TEM images, (D) electron diffraction pattern, and (E) XRD pattern of PdNPs synthesized by using acidic then alkaline-treated sucrose as a reducing agent .....	28
4.7 The mechanism of sucrose degradation under acidic condition.....	30
4.8 The mechanism of mutarotation and isomerization of monosaccharide to generate enediol anion intermediate.....	31
4.9 The mechanism of monosaccharides degradation under alkaline condition.....	32
4.10 A simplified reaction scheme of monosaccharides degradation under alkaline condition .....	33
4.11 ATR FT-IR spectra of (A) sucrose, (B) alkaline-treated sucrose, (C) acidic-treated sucrose, (D) acidic then alkaline-treated sucrose, and (E) PdNPs synthesized by using acidic then alkaline-treated sucrose as reducing agent.....	34
4.12 Optical images depicting the formation of Pd film at air-water interface .....	35
4.13 SEM micrographs of Pd film (A) lower and (B) higher magnifications, and (C) EDX spectrum.....	36
4.14 (A-F) SEM micrographs revealing evolution of Pd film formation at air-water interface .....	37
4.15 UV-vis spectra revealing the decrease of $\text{PdCl}_4^{2-}$ absorbance in 6 days after stopping the reaction .....	38
4.16 XRD pattern of Pd film .....	39

Figure	Page
4.17 Optical images depicting the evolution of FPd $\mu$ STs synthesizing by mixing 5.64 mM PdCl $_4^{2-}$ solution with 30% HP. The particle evolution was monitored through the scattering of a green laser pointer.....	39
4.18 SEM micrographs of FPd $\mu$ STs at (A) lower and (B) higher magnifications and (C) EDX spectrum .....	40
4.19 SEM micrographs of PdNPs and FPd $\mu$ STs synthesized using 15% HP with PdCl $_4^{2-}$ concentration of (A) 100, (B) 300, (C) 500, and (D) 1000 ppm .....	41
4.20 SEM micrographs of FPd $\mu$ STs synthesized using 400 ppm PdCl $_4^{2-}$ with HP concentration of (A) 5, (B) 15, (C) 25, and (D) 35 %.....	42
4.21 (A - E) SEM and (F - J) TEM images revealing evolution of FPd $\mu$ STs and the formation of FPd $\mu$ STs from PdNPs.....	43
4.22 The schematic diagram illustrates the formation mechanism of FPd $\mu$ STs.....	45
4.23 (A - D) SEM micrographs of Pd $\mu$ STs (minor structures) synthesized by using 15% HP and 100 ppm of PdCl $_4^{2-}$ .....	45
4.24 (A) TEM image, (B) electron diffraction pattern, and (C) XRD pattern of FPd $\mu$ STs.....	46

## LIST OF ABBREVIATIONS

Pd	: palladium
PdNPs	: palladium nanoparticles
FPd $\mu$ STs	: flowerlike palladium microstructures
HP	: hydrogen peroxide
mL	: milliliter
nm	: nanometer
$\mu$ m	: micrometer
V	: volt
eV	: electron volt
SEM	: scanning electron microscopy
TEM	: transmission electron microscopy
ATR FT-IR	: attenuated total reflection Fourier transform infrared
EDX	: energy dispersive X-ray
XRD	: X-ray diffraction
UV-vis	: ultraviolet-visible
IRE	: internal reflection element
MCT	: mercury-cadmium-telluride
PdCl $_4^{2-}$	: palladium chloride
NaBH $_4$	: sodium borohydride
NaOH	: sodium hydroxide
HCl	: hydrochloric acid
H $_2$ O $_2$	: hydrogen peroxide
$^{\circ}$ C	: degree Celsius
E $^0$	: redox potential
$\theta$	: theta
$\mu$	: micro
$\alpha$	: alpha
$\beta$	: beta
cm $^{-1}$	: wave number

# CHAPTER I

## INTRODUCTION

### 1.1 Nanotechnology

Nanotechnology is a term that is widely discussed and draws attention of scientists and people all over the world. Many definitions to describe the word “nanotechnology” have been made, but the most accepted definition is these three following attributes [1].

1. Research and technology development at the atomic, molecular or macromolecular levels, in the length scale of approximately 1 – 100 nanometer range.
2. Creating and using structures, devices and systems that have novel properties and functions because of their small and/or intermediate size.
3. Ability to control or manipulate on the atomic scale.

Nanotechnology has the ability to create many new materials and devices with many applications, such as medicine, electronics, and energy production. Therefore, there are many products, which we use in our daily life, involve with nanotechnology.

### 1.2 Nanomaterials and their catalytic usage

Due to special electronic, optical, and magnetic properties when compare to their bulk form, nanomaterials, which are one of the big part in nanotechnology, are interested in the materials world. Nanomaterials are used in electronic, biomedical, pharmaceutical, cosmetics, energy, and catalytic applications [2]. Industrial-scale production of some types of nanomatials such as carbon black nanoparticles, titanium dioxide nanoparticles, or polymer dispersions has been produced for a long time.

Catalytic usage is one of the foremost applications of nanomaterials. Various catalytic reactions, such as reforming, combustion, methanol synthesis, hydrogen and hydrogen peroxide production, CO and CO<sub>2</sub> hydrogenation, and Fischer-Tropsch

synthesis of fuel are receiving much more attention because of their important for petroleum and petrochemical industry, power generation, and pollution abatement [3]. During the past years, the preparation of catalyst from nanomaterials with a very high performance has been challenged. One of the important characteristics that nanomaterials catalyst should have is a high dispersion with narrow particle size distribution, especially for reactions which the final product distribution varies with the particle size of catalyst. Various kinds of metal, usually in the form of nanoparticles supported on substrate, have been used as a catalyst. For examples, palladium nanoparticles supported on  $ZrO_2$ ,  $TiO_2$ , or  $Al_2O_3$  (for methanol synthesis and hydrogen production), platinum nanoparticles deposited on carbon (for electrocatalysts), and  $TiO_2$  (for photocatalysts). These catalysts are called heterogeneous catalyst [3]. The major advantages of heterogeneous catalyst are that they are easy to separate from reactants and products and can be used at high temperature and pressure. However, the disadvantages are their poor catalytic activity and selectivity compared to homogeneous catalyst [4]. Therefore development on homogeneous catalyst becomes a more popular topic for the scientific research. Many methods have been used to synthesize metal nanoparticles for catalytic applications. However, most of the synthetic methods still use toxic and expensive chemicals as reducing agent, stabilizer and solvent. Moreover, some methods are complicated which consume a lot of energy and generate a lot of toxic wastes. Also the problem of toxic chemicals waste release in the environment which is a big global issue at the moment.

In this work, we have developed a novel green, efficient, and commercializable approach for synthesizing high-concentration palladium nanoparticles by using sucrose and hydrogen peroxide, which are very cheap and harmless to the environment, as both reducing and stabilizing agents. This approach can be scaled-up for the production of high-concentration palladium nanoparticles for industrial use with a highly competitive price.

### 1.3 The research objective

The objective of this research is to develop a novel method for the synthesis of high-concentration palladium nanoparticles by using sucrose and hydrogen peroxide as reducing agents.

### 1.4 The research scopes

1. Develop a novel method for the synthesis of high-concentration palladium nanoparticles by using sucrose and hydrogen peroxide as reducing agents.
2. Study effect of the synthetic parameters, which are the acidic and alkaline treatments of sucrose, concentration of reducing agent, and concentration of palladium chloride precursor, on the particle morphology.
3. Investigate the morphology (size, shape and crystal structure) of synthesized palladium nanoparticles by scanning electron microscope, transmission electron microscope, and X-ray diffractometer.
4. Investigate the functional group transformations of sucrose after acidic and alkaline treatments by attenuated total reflection Fourier transform infrared spectroscopy.

### 1.5 Benefit of research

Obtain green, efficient, and commercializable approach for the synthesis of high-concentration palladium nanoparticles using sugar and hydrogen peroxide as reducing agents.



## CHAPTER II

### THEORETICAL BACKGROUND

#### 2.1 Properties and applications of palladium

Palladium is a silvery-white, ductile, and malleable metal which was discovered in 1803 by William Hyde Wollaston during the process of platinum refining. It was named after the newly discovered asteroid, Pallas which is the name of the Greek goddess of wisdom. The major sources of palladium are located in South Africa and Russia [5].

Palladium is one of the noble metals in the platinum group elements (PGEs) which comprising of the rare platinum (Pt), palladium (Pd) rhodium (Rh), ruthenium (Ru), iridium (Ir), and osmium (Os). Palladium is a noble metal which is difficult to oxidize because of a combination of high sublimation energy and high ionization potential [5]. The most important application of palladium is using as a catalyst. Palladium is widely used as a catalyst for various purposes, especially in petroleum and petrochemical industry that needs to accelerate chemical processes in order to save energy, time, and chemical usage. Palladium is used as the catalysts in various organic reactions such as petroleum cracking process, Suzuki coupling reaction [6], and hydrogenation [7, 8] (Figure 2.1B). The highest demand of palladium comes from the manufacturing of automobile catalytic converter in automobile industry which palladium catalyst converts pollutants in engine exhaust gases into harmless non-pollutants [9] (Figure 2.1A). According to its ability in absorbing hydrogen (up to 900 times of its own volume) [10], palladium is used as a catalyst in hydrogen gas fuel cell [11] (Figure 2.2) which is one of the important energy source in the future.

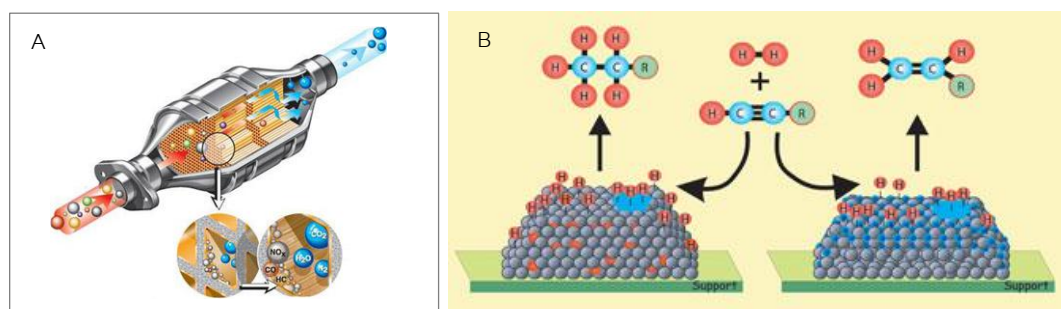


Figure 2.1 Applications of palladium catalyst for automobile catalytic converter [12] (A) and hydrogenation reaction [8] (B).

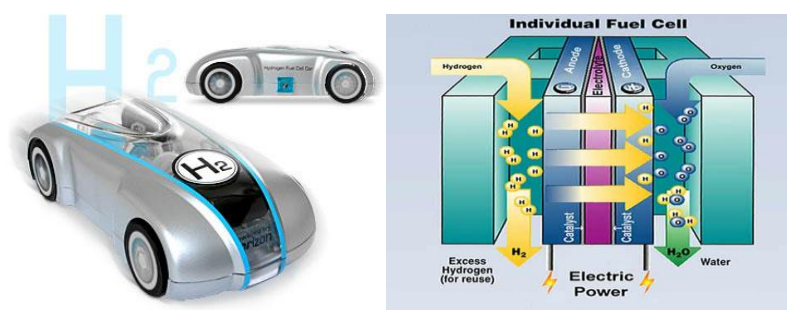


Figure 2.2 Applications of palladium catalyst for hydrogen gas fuel cell [13].

Palladium can be made into finely divided forms, especially the nanoparticles that are catalytically active. Nowadays, research on palladium nanoparticles (PdNPs) synthesis are not only focused on production of very small size PdNPs (i.e., in order to enhance catalytic activity via high surface area) [14], but also paying attention to the shape-control synthesis of PdNPs (i.e., in order to enhance catalytic activities via shape effect) [14-16].

## 2.2 Synthesis of palladium nanoparticles

Methods for the synthesis of PdNPs could be divided into two distinct ways which are physical method and chemical method (Figure 2.3). Physical method is based on the breaking down of bulk metals and subsequent stabilization of the generating nanoparticles by addition of surfactant or capping agents. The examples of technique used in this physical method are laser ablation, focused ion beam milling and electron beam lithography (Figure 2.4). On the other hand, chemical method is based on the growth of nanoparticles starting from metal atoms, which are obtained

from ionic precursors [17]. The most well-known technique in this chemical method is chemical reduction (Figure 2.5). The latter method is likely to be more popular because it is simple and no need for an advanced instrument to fabricate nanoparticles. The chemical reduction generally involves reducing agent that gives the electron to metal ion to form zero-valent metal atom which then nucleate and growth into metal nanoparticles. The examples of chemical, which commonly used as a reducing agent, are sodium borohydride ( $\text{NaBH}_4$ ), hydrazine ( $\text{N}_2\text{H}_4$ ), and alcohol. However, the naked metal nanoparticles are unstable and have a tendency to aggregate and precipitate out which make them lose their catalytic activities. Therefore metal nanoparticles need to be stabilized or surface-protected by stabilizing or capping agent which can be uniformly dispersed in organic solvents or water. The examples of chemical, which commonly used as stabilizing or capping agent, are polymer and surfactant [18].

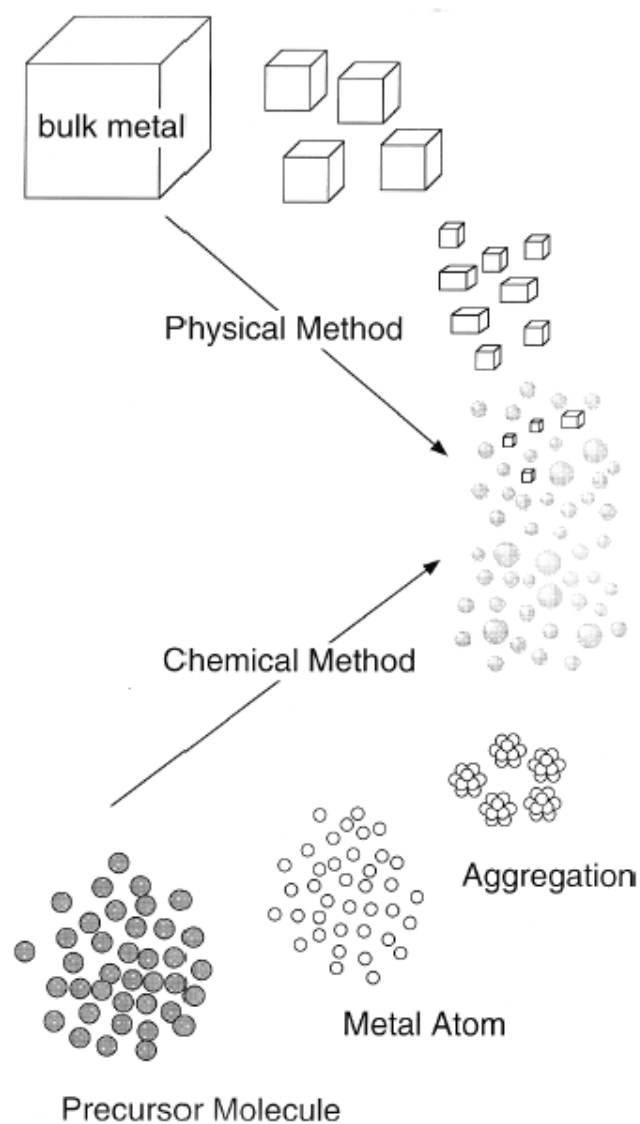


Figure 2.3 Schematic illustration of metal nanoparticles preparation by physical and chemical methods [17].

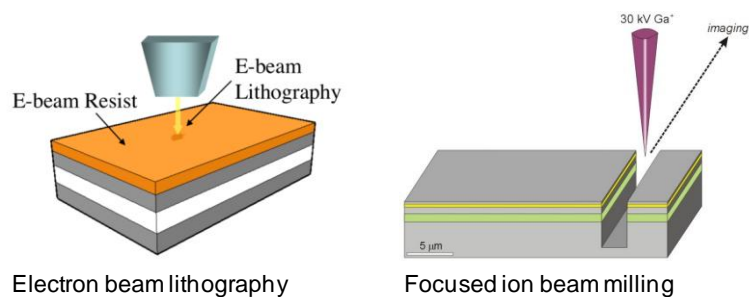


Figure 2.4 Techniques [19, 20] for synthesis of metal nanoparticles by physical method.

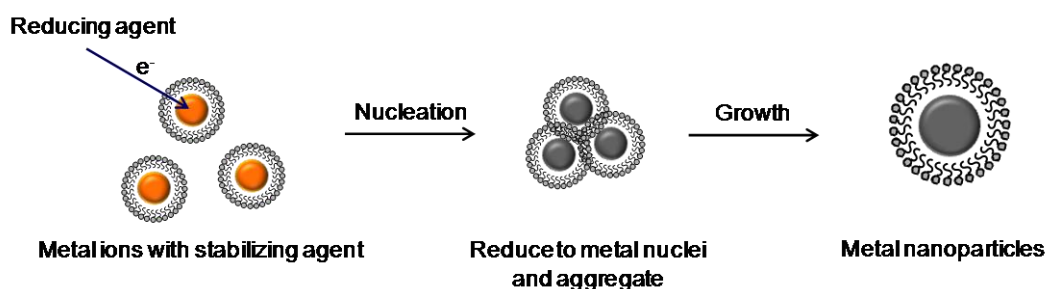
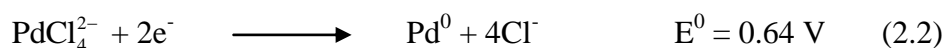


Figure 2.5 Synthesis of metal nanoparticles by chemical reduction [18].

### 2.3 Synthesis of palladium nanoparticles by chemical reduction

For the synthesis of PdNPs by chemical reduction, the palladium ion ( $\text{Pd}^{2+}$ ) is usually in the stable form of palladium chloride complex ( $\text{PdCl}_4^{2-}$ ). However, due to a higher reduction potential, the reduction of  $\text{Pd}^{2+}$  is faster than  $\text{PdCl}_4^{2-}$ . The reduction of  $\text{Pd}^{2+}$  and  $\text{PdCl}_4^{2-}$  to  $\text{Pd}^0$  metal can be described by equation 2.1 [21] and 2.2 [22].



Many methods have been developed for the synthesis of PdNPs by chemical reduction. These methods are mostly different in the chemicals used as reducing and stabilizing agent, solvent, and synthetic condition which are the temperature, pressure, and catalyst. Also the resulting PdNPs are different in morphologies which are size and shape of the nanoparticles. The examples of research about synthesis of PdNPs are presented as follows:

In 1998, Teranishi and Miyake [23] synthesized PdNPs by using alcohol as a reducing agent and polyvinylpyrrolidone (PVP) as a stabilizer. The final concentration of synthesized PdNPs is 90 ppm. The synthesized nanoparticles are spherical shape with the particles size of 1.7 to 3 nm. The size of nanoparticles could be reduced by increasing the concentration of reducing and stabilizing agents.

In 2001, Yonezawa et al. [24] synthesized PdNPs by using hydrazine as a reducing agent and quaternary ammonium salt alkylisocyanides as a stabilizer. The

final concentration of synthesized PdNPs is 200 ppm. The shape of nanoparticles is spherical with particles size of 3 to 10 nm. In this work, the stabilizer used is a cationic surfactant with the hydrophilic chain. Therefore the stabilized nanoparticles could well disperse in water. Moreover, the size of nanoparticles could be reduced by increasing the hydrophilic chain-length of surfactant.

One of the most referenced publications is the work of Kim et al. in 2005 [25], which PdNPs were synthesized by using acetylacetonate as a reducing agent and trioctylphosphine as a stabilizer. The concentration of synthesized nanoparticles is 3000 ppm. The spherical PdNPs with the particle size of 3.5 to 7 nm were obtained. The thermal decomposition at 250 °C was believed to be the catalyst for generating reducing property acetylacetonate.

In addition to develop the method for synthesis of PdNPs, the utilization of the synthesized PdNPs as a catalyst was also studied by many research. In 2004, Pillai and Demessie [7] synthesized PdNPs by using polyethylene glycol as a reducing agent and phenanthroline as a stabilizer. The spherical PdNPs with the size of 2 to 6 nm were obtained. The final concentration of PdNPs is 100 ppm. The obtained nanoparticles were applied as a catalyst for the hydrogenation reaction of olefin. They found that the catalytic activity of PdNPs stabilized by phenanthroline is better than the one with no phenanthroline stabilized.

Beyond the synthesis of spherical shape of PdNPs, methods for shape-controlled synthesis, to obtain others shape of PdNPs with a better activity and selectivity for catalytic usage, were also developed. In 2007, Chang et al. [16] synthesized PdNPs by using ascorbic acid as a reducing agent and cetyltrimethylammonium bromide (CTAB) as a stabilizer. The concentration of PdNPs is 30 ppm. The shape and size of the nanoparticles is cubic and 85 nm (Figure 2.6), respectively. In this work, CTAB played an important role for controlling the growth of nanoparticles into cubic shape by selectively stabilized on the crystal facet and slowed down the rate of nanoparticles growth.

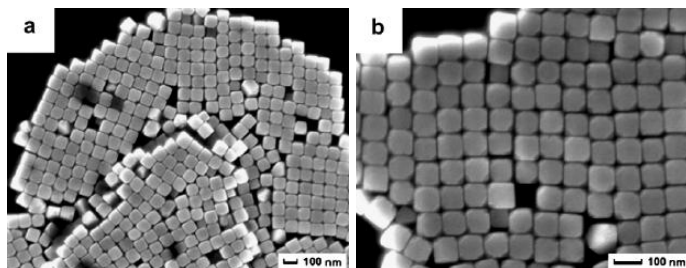


Figure 2.6 Cubic shape of PdNPs with the size of 85 nm [16].

There are many other researchers developed methods for the shape-controlled synthesis of PdNPs by using CTAB as stabilizing and shape-controlling agents. The other shapes of PdNPs unless cubic were successfully synthesized. In 2010, Niu et al. [10] synthesized PdNPs by using ascorbic acid as a reducing agent and CTAB as a stabilizer. The concentration of synthesized nanoparticles is 25 ppm. The PdNPs with many shapes such as dodecahedral, decahedral, and rod-shaped were obtained (Figure 2.7). The particle size is 100 nm. The highlight of this work is the use of potassium iodide (KI) for controlling the growth of PdNPs into many shapes. Moreover, increase the synthetic temperature could result in a shape of PdNPs with more edge and corner.

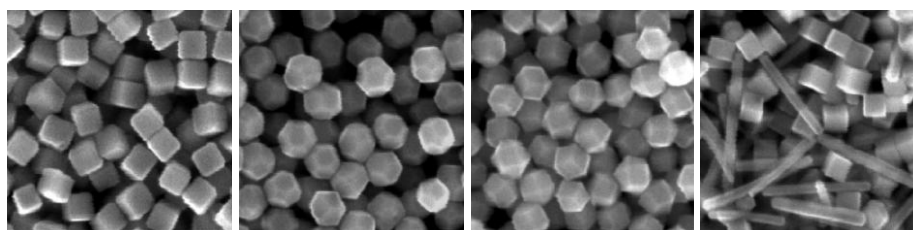


Figure 2.7 Cubic, decahedral, octahedral, and rod shapes of PdNPs [10].

Although the above mentioned succeed to develop many methods for the synthesis of PdNPs with a high potential to be used as a catalyst. However, most of these synthetic methods still use toxic and expensive chemicals as reducing agent, stabilizer and solvent. Moreover, these methods are complicated which consume a lot of energy and generate a lot of toxic wastes. Also the problem of toxic chemicals waste release in the environment which is a big global issue at the moment. Therefore the 12 principles of green chemistry [26] were established for science and technology development. These principles are basically about design of processes which are

maximize the amount of raw material that ends up in the product, use of safe and environmental-friendly substances, and energy efficient use.

The 12 principles of green chemistry become interested by many researches focusing on the synthesis of PdNPs. The researchers try to use chemicals which are non-toxic and environmental-friendly as reducing and stabilizing agents. In 2004, Panigrahi et al. [27] synthesized palladium nanoparticle by using glucose, fructose, and sucrose as reducing as well as stabilizing agents. The concentration of synthesized PdNPs is 25 ppm. The spherical PdNPs with the size in the range of 1 to 20 nm were obtained. In this work, it was found that sucrose which is a non-reducing sugar can be used as a reducing agent because sucrose was hydrolyzed under acidic condition to yield glucose and fructose which are both reducing sugars.

Twelve principles of green chemistry are listed as follows:

1. Prevent waste
2. Atom economy
3. Less hazardous chemical synthesis
4. Designing safer chemicals
5. Safer solvents/reaction media
6. Design for energy efficiency
7. Renewable feedstocks
8. Reduce derivatives
9. Catalysis
10. Design for degradation/design for end of life
11. Real-time monitoring and process control
12. Inherently safer chemistry

In 2007, Nadagouda and Varma [28] synthesized PdNPs by using vitamin B2 as reducing as well as stabilizing agents. The synthesized nanoparticles are in the concentration of 1000 ppm. The spherical and rod-shaped PdNPs with the size in the range of 5 to 13 nm were obtained. The size and shape of nanoparticles could be controlled by changing the type of solvent used.



It was found that the size of PdNPs could be reduced by increasing the rate of nucleation of nanoparticles. In 2009, He et al. [21] synthesized PdNPs by using ascorbic acid as a reducing agent and carboxymethyl cellulose (CMC) as a stabilizer. The final concentration of synthesized nanoparticles is 20 ppm. The size and shape of nanoparticles are 3.6 nm and spherical, respectively. In this work, increasing the synthetic temperature could increase the rate of nucleation which resulted in a smaller size of PdNPs. Moreover, CMC played an important role as a stabilizing agent by reduced the kinetic energy of nanoparticles. Therefore very small size PdNPs with a narrow size distribution were obtained.

There is also the synthesis of PdNPs by using plant-extracted as a reducing agent. In 2009, Yang et al. [29] synthesized PdNPs by using broth of *C.camphora* leaf as reducing as well as stabilizing agents. The synthesized PdNPs are in the concentration of 500 ppm. The spherical PdNPs with the size of 3.2 to 6 nm were obtained. The smaller size PdNPs with a narrow size distribution were obtained by increasing the concentration of used palladium chloride. They explained that the rate of nucleation was increases while the Oswald ripening process was inhibited by increasing the concentration of used palladium chloride.

Furthermore in 2009, Liu et al. [9] synthesized PdNPs by using ascorbic acid as a reducing agent and chitosan as a stabilizer. The synthesized PdNPs are in the concentration of 20 ppm. The polyhedral and flowerlike PdNPs with the size of 60 to 70 nm were obtained (Figure 2.8). The synthesized nanoparticles were also applied as a surface enhanced Raman substrate. It was found that the flowerlike PdNPs had a higher Raman enhancement factor than the polyhedral shape.

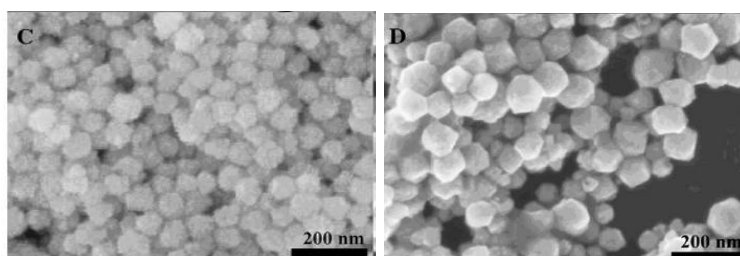


Figure 2.8 Flowerlike and polyhedral shapes of PdNPs with the size of 60 nm [9].

All of these researches suggest that PdNPs could be synthesized by using various kinds of reducing and stabilizing agent which are non-toxic and friendly to

environment. However, there are a few researches synthesized PdNPs at a high concentration. In this work, we try to develop a new method for the synthesis of PdNPs by using sucrose and hydrogen peroxide, which are harmless to environment, as reducing agents. Sucrose can be bought from a local supermarket with a very low price. Moreover, we synthesized PdNPs from palladium chloride which prepared by dissolving palladium metal in aqua regia. Therefore we could save the cost by 40 times comparing to that buying palladium chloride from commercial.

#### 2.4 Theory on nucleation and growth of metal nanoparticles

In the typical synthesis of metal nanoparticles, the formation of the nanoparticles could be explained by the nucleation and growth mechanism proposed by Lamer and co-workers [30] (Figure 2.9). The first step involves the reduction of metal ion precursor, which usually in the form of metal salt, into zero-valent metal atom. For the synthesis of PdNPs, the most commonly precursor used is  $\text{PdCl}_4^{2-}$  which can be reduced to Pd atoms by a reducing agent. When the concentration of Pd atoms is high enough to reach the critical limit of supersaturation, the Pd atoms aggregate to form nuclei by the nucleation process. These nuclei then grow by addition of atoms to the nuclei which result in the drop of concentration of Pd atoms. When the concentration of atoms decreases below the level of minimum supersaturation, no additional nucleation can occur and the nuclei can continue to grow via supply of atoms in the solution. The nuclei will grow into larger size nanocrystals until equilibrium has been reached. Besides this, nuclei and nanocrystals can undergo agglomeration and merge into larger objects.

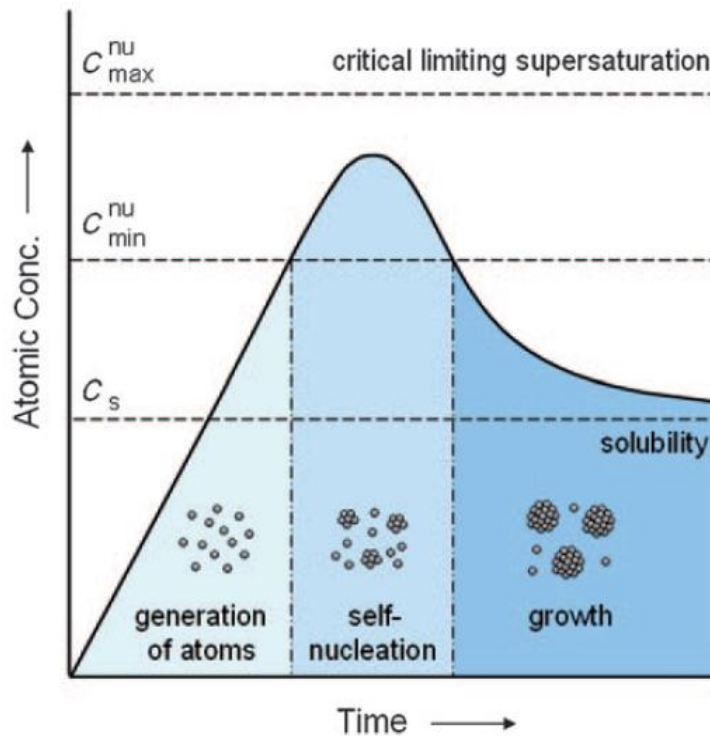


Figure 2.9 Plot of atom concentration and time, showing the nucleation and subsequent growth [30].

## 2.5 Stabilization of metal nanoparticles

Polymer or surfactant is often used as stabilizers of metal nanoparticles. These substances can control both reduction rate of metal ions and the aggregation process of metal atoms. Typically, there are two types of stabilization which are electrostatic stabilization and steric stabilization [2, 31].

Electrostatic stabilization is the adsorption of ions to the electrophilic metal surface. The electrical double layers of adsorption are created. These double layers result in a Coulombic repulsion force between individual particles (Figure 2.10).

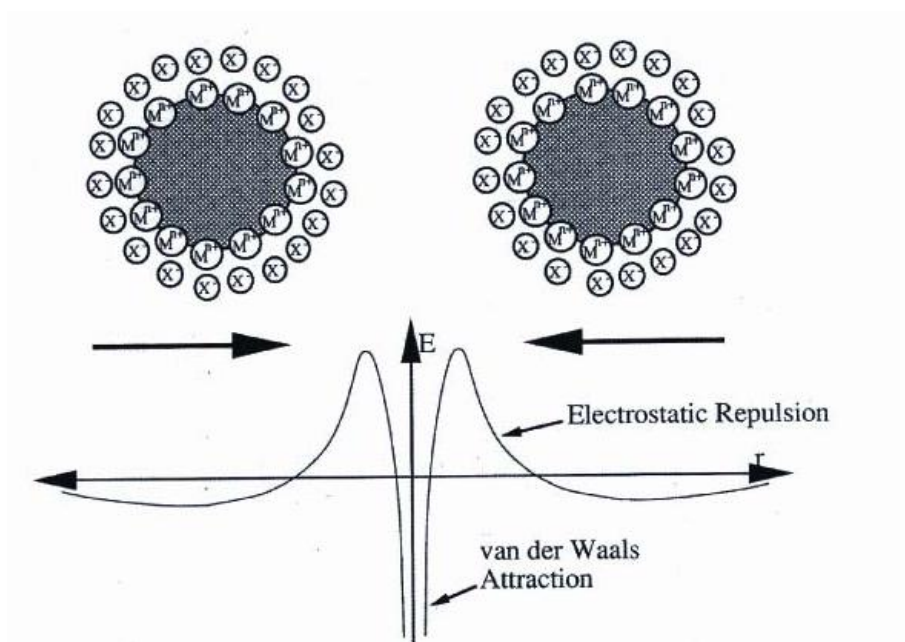


Figure 2.10 Schematic illustration of metal nanoparticles stabilized by electrostatic repulsion [2].

Another method is the steric stabilization which molecule of polymer or surfactant adsorb on the metal nanoparticles surface. These molecules adsorbed on the surface of nanoparticles generate a steric barrier which inhibits the aggregation between nanoparticles (Figure 2.11).

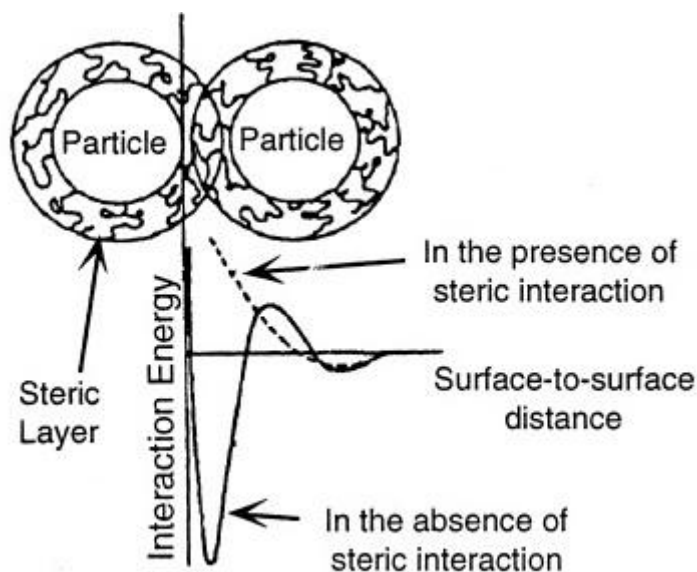


Figure 2.11 Schematic illustration of metal nanoparticles stabilized by steric hindrance [31].

## CHAPTER III

### EXPERIMENT

#### 3.1 Chemicals and materials

Palladium chloride ( $\text{PdCl}_4^{2-}$ ) solution was prepared by dissolving 10 g of palladium metal in 50 mL of aqua regia [32]. The solution was stirred under gentle heat until palladium metal was completely dissolved. The volume adjustment was made in order to obtain a certain concentration (100,000 ppm) of  $\text{PdCl}_4^{2-}$  solution. Sucrose was bought from local supermarket. Other chemicals used in this experiment are all of an analytical grade (Merck, Germany). All chemicals were used as-received without further purification. The de-ionized water was used as solvent.

#### 3.2 Synthesis of palladium nanoparticles by using sucrose as a reducing agent

Palladium nanoparticles (PdNPs) were prepared via reduction of  $\text{PdCl}_4^{2-}$  by sucrose. A 10 mL of 1% (w/v) sucrose solution was heated at 90 – 100 °C for 15 min. Then, 10 mL of 2000 ppm  $\text{PdCl}_4^{2-}$  was rapidly added under vigorous stirring and was allowed to be proceeded for a reduction reaction at 90 – 100 °C for 15 min. The color of the solution gradually turned slightly black after the  $\text{PdCl}_4^{2-}$  addition, indicating the formation of PdNPs.

### 3.3 Synthesis of palladium nanoparticles by using acidic and alkaline-treated sucrose as reducing agents

The effect of acidic and alkaline treatment on the reducing property of sucrose was studied. Sucrose was treated with hydrochloric acid (HCl) and sodium hydroxide (NaOH) before using as a reducing agent. The treatment process was divided into 3 categories, which are acidic-treatment, alkaline-treatment, and acidic then alkaline-treatment.

#### 3.3.1 Synthesis of palladium nanoparticles by using acidic-treated sucrose as a reducing agent

For the synthesis of PdNPs by using acidic-treated sucrose as a reducing agent, a 50 mL of 2% (w/v) sucrose was heated with 10 mL of 1 M HCl at 90 – 100 °C for 30 min. Then, the solution was cooled down to room temperature and pH was adjusted to 7 by 0.2 M NaOH. The volume was adjusted back to 50 mL in order to obtain a 2% (w/v) of acidic-treated sucrose solution.

A 10 mL of 1% (w/v) acidic-treated sucrose solution was heated at 90 – 100 °C for 15 min. Then, a 10 mL of 2000 ppm  $\text{PdCl}_4^{2-}$  was rapidly added under vigorous stirring and was allowed to be proceeded for a reduction reaction at 90 – 100 °C for 15 min. The color of the solution gradually turned slightly black after the  $\text{PdCl}_4^{2-}$  addition, indicating the formation of PdNPs.

#### 3.3.2 Synthesis of palladium nanoparticles by using alkaline-treated sucrose as a reducing agent

For the synthesis of PdNPs by using alkaline-treated sucrose as a reducing agent, a 5 mL of 2% (w/v) sucrose was heated with 5 mL of 0.2 M NaOH at 90 – 100 °C for 15 min. Then, 10 mL of 2000 ppm  $\text{PdCl}_4^{2-}$  was rapidly added under vigorous stirring and was allowed to be proceeded for a reduction reaction at 90 – 100 °C for 15 min. The color of the solution gradually turned black after the  $\text{PdCl}_4^{2-}$  addition, indicating the formation of PdNPs.

### 3.3.3 Synthesis of PdNPs by using acidic then alkaline-treated sucrose as a reducing agent

For the synthesis of PdNPs by using acidic then alkaline-treated sucrose as a reducing agent, a 50 mL of 2% (w/v) sucrose was heated with 10 mL of 1 M HCl at 90 – 100 °C for 30 min. Then, the solution was cooled down to room temperature and pH was adjusted to 7 by 0.2 M NaOH. The volume was adjusted back to 50 mL in order to obtain a 2% (w/v) of acidic-treated sucrose solution.

A 10 mL of 1% (w/v) acidic-treated sucrose solution was heated with 5 mL of 0.2 M NaOH at 90 – 100 °C for 15 min. The color of the solution gradually changed from colorless to orange. Then, a 10 mL of 2000 ppm  $\text{PdCl}_4^{2-}$  was rapidly added under vigorous stirring and was allowed to be proceeded for a reduction reaction at 90 – 100 °C for 15 min. The color of the solution suddenly turned black after the  $\text{PdCl}_4^{2-}$  addition, indicating the formation of PdNPs.

## 3.4 Preparation of palladium film through self-assembly of palladium nanoparticles at air-water interface

Palladium (Pd) film was prepared by the self-assembly of PdNPs synthesized by using acidic then alkaline-treated sucrose as a reducing agent. Self-assembly of PdNPs at air-water interface occurred only when a high concentration of  $\text{PdCl}_4^{2-}$  was employed. The process is the same as the synthesis of PdNPs by using acidic then alkaline-treated sucrose as reducing agent (3.3.3). The only one difference was the concentration of  $\text{PdCl}_4^{2-}$ , which 10,000 ppm of  $\text{PdCl}_4^{2-}$  was used instead of 2,000 ppm. Pd film gradually appeared and became more apparent within two days after the reaction.

### 3.5 Synthesis of flowerlike palladium microstructures by using hydrogen peroxide as a reducing agent

Flowerlike palladium microstructures (FPd $\mu$ STs) were synthesized via reduction of PdCl<sub>4</sub><sup>2-</sup> by hydrogen peroxide (HP) under an acidic condition. Briefly, 5 mL of 30% HP was rapidly added into 5 mL of 600 ppm PdCl<sub>4</sub><sup>2-</sup> solution. The solution was homogeneously mixed before left standing undisturbed throughout the course of reaction. The particles precipitated after a prolonged standing for 30 min. The particles were separated via decantation and filtration.

### 3.6 Characterization of palladium nanoparticles, palladium film, and flowerlike palladium microstructures

The synthesized PdNPs, Pd film, and FPd $\mu$ STs were characterized by a variety of techniques. The completion of reaction was observed by UV-vis spectroscopy. The particle morphology was investigated by scanning electron microscope (SEM) and transmission electron microscope (TEM). Attenuated total reflection Fourier transform-infrared (ATR FT-IR) microspectroscopy was applied for monitoring the functional group transformations of sucrose after acidic and alkaline treatments. Crystal structure was observed by X-ray diffraction (XRD) technique.

#### 3.6.1 UV-vis spectroscopy

The UV-vis spectra were obtained on Mikropack DH-2000 UV-vis NIR spectrometer with Spectra Suit software. The deuterium lamp with a scan range of 200 - 850 nm was used as a light source. The quartz cuvette with optical path length of 1.0 cm was employed as a sample cell. All UV-vis spectra were referenced using de-ionized water.



### 3.6.2 Scanning electron microscopy

The SEM micrographs were recorded using JEOL JSM-6510A scanning electron microscope, operating at 20 and 30 keV. The colloidal PdNPs were centrifuged at 4000 rpm for 10 min to obtain black precipitate. The precipitate was washed with de-ionized water for several times and then re-dispersed in de-ionized water under ultra sonic for 10 min. The purified PdNPs were then deposited on the plastic sheet by centrifugation at 4000 rpm for 10 min. The deposited particles were picked-up by a carbon-tape attaching on the aluminum stub and ready for SEM characterization.

### 3.6.3 Transmission electron microscopy

The TEM images were recorded using FEI Tecnai™ G<sup>2</sup> 20 S-TWIN transmission electron microscope operated at 200 keV. The colloidal PdNPs were centrifuged at 4000 rpm for 10 min to obtain black precipitate. The precipitate was washed with de-ionized water for several times and then re-dispersed in de-ionized water under ultra sonic for 10 min. The purified PdNPs were then deposited on a copper grid and ready for TEM characterization.

### 3.6.4 Attenuated total reflection Fourier transform infrared spectroscopy

The IR spectra were record using Nicolet 6700 FT-IR spectrometer with an attenuated total reflection (ATR) technique. Germanium was used as an internal reflection element (IRE). The mercury-cadmium-telluride (MCT) was used as a detector. The sample was dropped-dried on the glass-slide and ready for ATR FT-IR characterization.

### 3.6.5 XRD technique

The XRD patterns were recorded by a DMAX 2200 Rigaku X-ray diffractometer equipped with a Cu K $\alpha$  radiation. The sample was dropped-dried on the glass-slide. After that, the dried samples in the form of powder or film were transferred to the XRD sample holder and ready for characterization.

## CHAPTER IV

### RESULTS AND DISCUSSION

#### 4.1 Palladium nanoparticles synthesized by using sucrose as a reducing agent

##### 4.1.1 Formation of palladium nanoparticles

PdNPs were synthesized via reduction of  $\text{PdCl}_4^{2-}$  by sucrose. In order to enhance the reducing efficiency, sucrose was pre-treated under acidic and alkaline conditions. The sucrose treatment was divided into 3 processes which are acidic, alkaline, and acidic then alkaline. Finally, PdNPs were obtained by 4 synthetic conditions. The optical image (Figure 4.1) shows that PdNPs synthesized by using sucrose (Figure 4.1A) and acidic-treated sucrose (Figure 4.1C) as reducing agents, have a yellow solution with a small amount of precipitated particles. These indicated that small amount of nanoparticles are obtained while a large amount of  $\text{PdCl}_4^{2-}$  are remained. On the other hand, PdNPs synthesized by using alkaline-treated sucrose (Figure 4.1B) and acidic then alkaline-treated sucrose (Figure 4.1D) as reducing agents, have a yellow-black solution with a large amount of precipitated particles and fully-black color, respectively. These indicated that large amount of nanoparticles are obtained. These results inform that alkaline treatment is a key factor for enhancing the reducing efficiency of sucrose. Therefore, a large amount of PdNPs are obtained. Moreover, PdNPs, synthesized by using acidic then alkaline-treated sucrose as a reducing agent, has the most dispersive property.

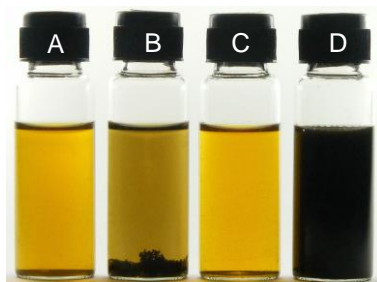


Figure 4.1 PdNPs synthesized by using (A) sucrose, (B) alkaline-treated sucrose, (C) acidic-treated sucrose, and (D) acidic then alkaline-treated sucrose as reducing agents.

#### 4.1.2 UV-vis absorption spectra of palladium nanoparticles

The UV-vis spectra of PdNPs, synthesized by using sucrose, alkaline-treated sucrose, acidic-treated sucrose, and acidic then alkaline-treated sucrose as reducing agents, were collected (Figure 4.2). The highest absorbance in the range of 300 to 700 nm, which is due to the absorption of black PdNPs [18], belongs to the PdNPs synthesized by using acidic then alkaline-treated sucrose as a reducing agent. This informs the presence of highly-disperse PdNPs colloid. The absorption in the 300 to 700 nm region is also found in PdNPs synthesized by using alkaline-treated sucrose as a reducing agent. The lower absorbance comparing to the PdNPs synthesized by using acidic then alkaline-treated sucrose as a reducing agent confirms the nanoparticles aggregations presented in PdNPs synthesized by using alkaline-treated sucrose as a reducing agent. On the other hand, the absorption in this region is not found in the PdNPs synthesized by using sucrose and acidic-treated sucrose as reducing agents. Nevertheless, there is the absorption peak around 240 nm which indicates the remaining of  $\text{PdCl}_4^{2-}$ . This absorption peak is not found in the absorption spectra of PdNPs synthesized by using alkaline-treated and acidic then alkaline-treated sucrose as reducing agents. However, there is also the absorption in the 240 to 350 nm region which belongs to the sucrose treated in acidic then alkaline solution. This absorption region overlaps with the absorption peak of  $\text{PdCl}_4^{2-}$ . Therefore, to make sure that there was no  $\text{PdCl}_4^{2-}$  remained, 0.1 M  $\text{NaBH}_4$  which is a very strong reducing agent was added into the PdNPs colloids. If there is a remained  $\text{PdCl}_4^{2-}$ , the

absorption in the 300 to 700 nm region would increase due to the formation of PdNPs from the reduction of  $\text{PdCl}_4^{2-}$ . After the addition of  $\text{NaBH}_4$ , the increase of absorption in the 300 to 700 nm region appears for PdNPs synthesized by using sucrose and acidic-treated sucrose as reducing agents (Figure 4.3A and 4.3C). On the other hand, there is no significantly increase of absorption in the 300 to 700 nm region for PdNPs synthesized by using alkaline-treated and acidic then alkaline-treated sucrose as reducing agents (Figure 4.3B and 4.3D). These results suggest that alkaline-treated and acidic then alkaline-treated sucrose are efficient reducing agents which could reduce all of  $\text{PdCl}_4^{2-}$  to PdNPs whereas sucrose and acidic-treated sucrose could not. It is concluded that alkaline is an important factor for the generation of sucrose reducing property.

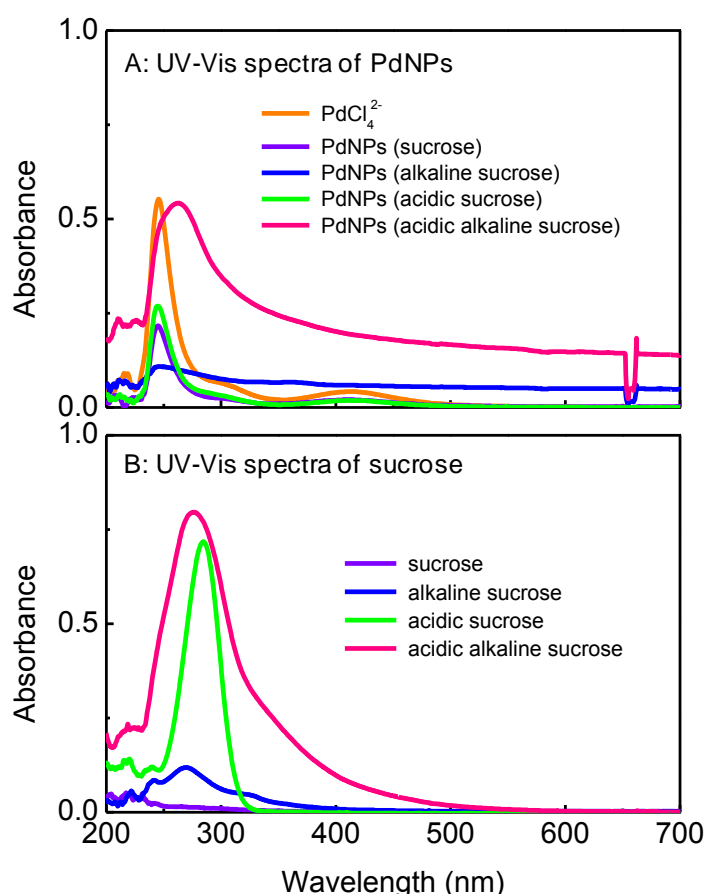


Figure 4.2 UV-vis spectra of (A) PdNPs synthesized by using sucrose treated in various conditions as reducing agents and (B) sucrose treated in various conditions.

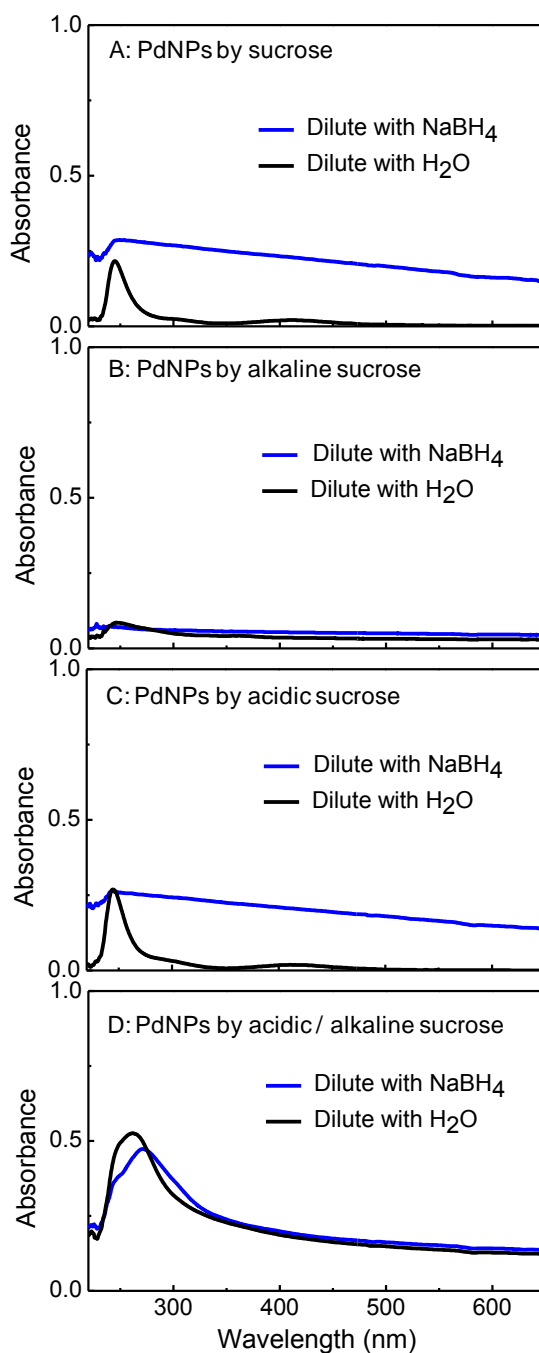


Figure 4.3 UV-vis spectra of PdNPs synthesized by using (A) sucrose, (B) alkaline-treated, (C) acidic-treated sucrose, and (D) acidic then alkaline-treated sucrose as reducing agents comparing between diluting with NaBH<sub>4</sub> (blue) and DI water (black).

#### 4.1.3 Morphology of palladium nanoparticles synthesized by using sucrose as a reducing agent

The morphology of PdNPs was investigated by SEM and the results are shown in Figure 4.4. Although acidic and alkaline treatments could affect the reducing efficiency of sucrose, they did not affect much to the morphology of the synthesized PdNPs. The size of PdNPs synthesized by using original, alkaline-treated, acidic treated, and acidic then alkaline treated sucrose as reducing agents is all in the range of 50 to 100 nm. The shape of the nanoparticles is nearly spherical with a number of aggregations. The reason why there are no difference of the particle morphology and a number of aggregations could be explained by the limitation of sucrose usage. Although the reducing efficiency of sucrose could be increased by pre-treating with acid and alkaline solution, the stabilizing property of sucrose is still poor. Sucrose is short chain disaccharides which likely to have less stabilizing power comparing to a long chain polymer or surfactant. Therefore, the synthesized nanoparticles would have more chance to aggregate together. Moreover, this organic molecule has a very strong interaction with the PdNPs which made it very difficult to be removed from the nanoparticles surface. This would be one reason for the aggregations of PdNPs because the organic molecule on particle surface could interact with the other one on other particle surface [33]. However, PdNPs synthesized by using acidic then alkaline- treated sucrose as a reducing agent seem to have more uniformity in size and shape than PdNPs synthesized by using sucrose treated by other three conditions as reducing agent.

The EDX measurement was performed to investigate the elemental composition of the particles. The intense peak at 2.85 keV indicating that PdNPs synthesized by using acidic then alkaline treated sucrose as reducing agent are dominantly composed of Pd metal (Figure 4.5C). The carbon (C) element in the EDX-spectrum originated from the employed carbon tape substrate.

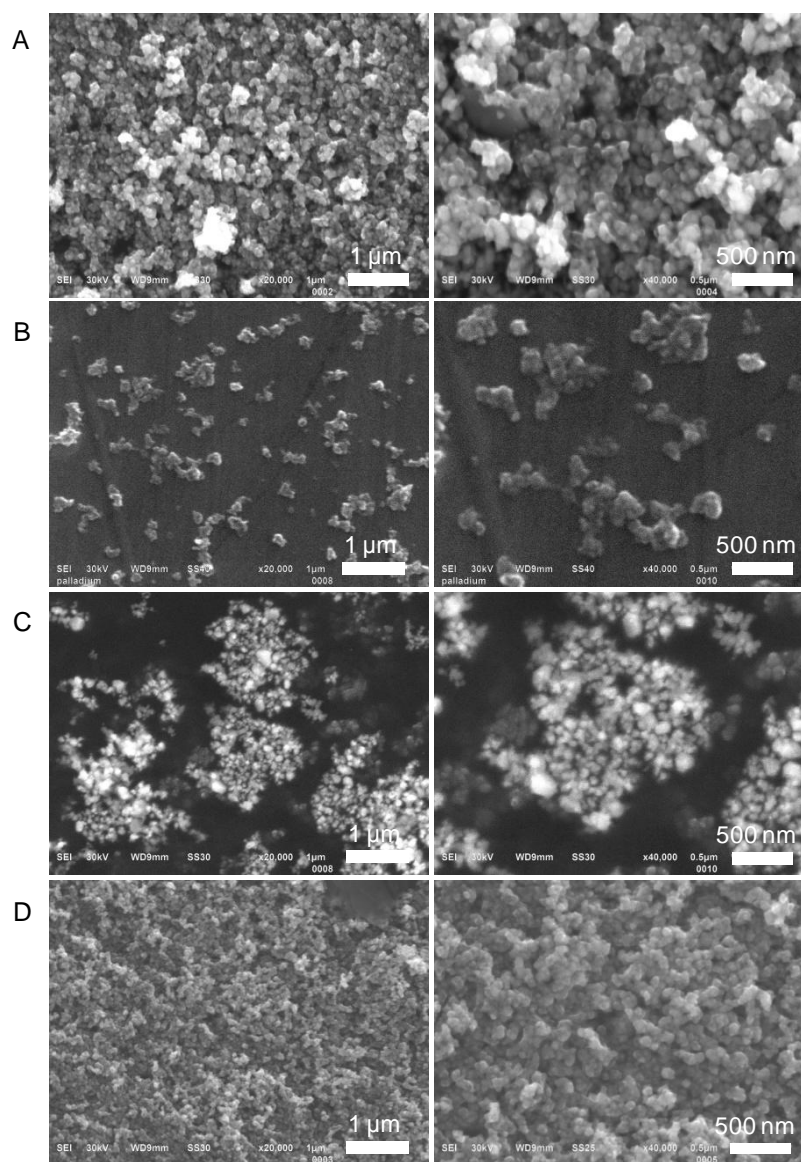


Figure 4.4 SEM micrographs of PdNPs synthesized by using (A) sucrose, (B) alkaline-treated, (C) acidic-treated sucrose, and (D) acidic then alkaline-treated sucrose as reducing agents. (left and right views are lower and higher magnifications, respectively)

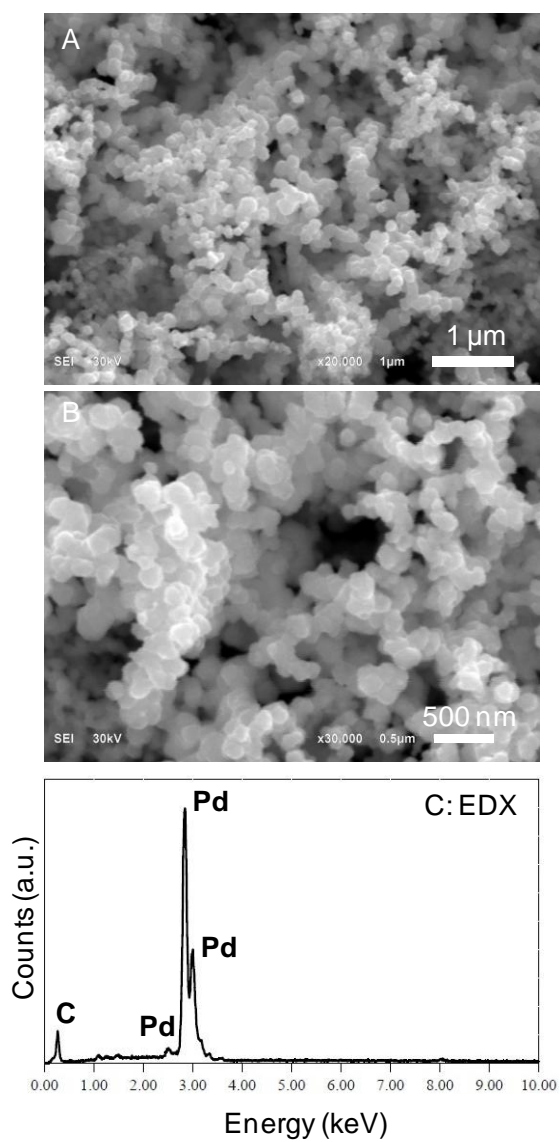


Figure 4.5 SEM micrographs of PdNPs synthesized by using acidic then alkaline-treated sucrose as a reducing agent, at (A) lower and (B) higher magnifications, and (C) EDX spectrum.



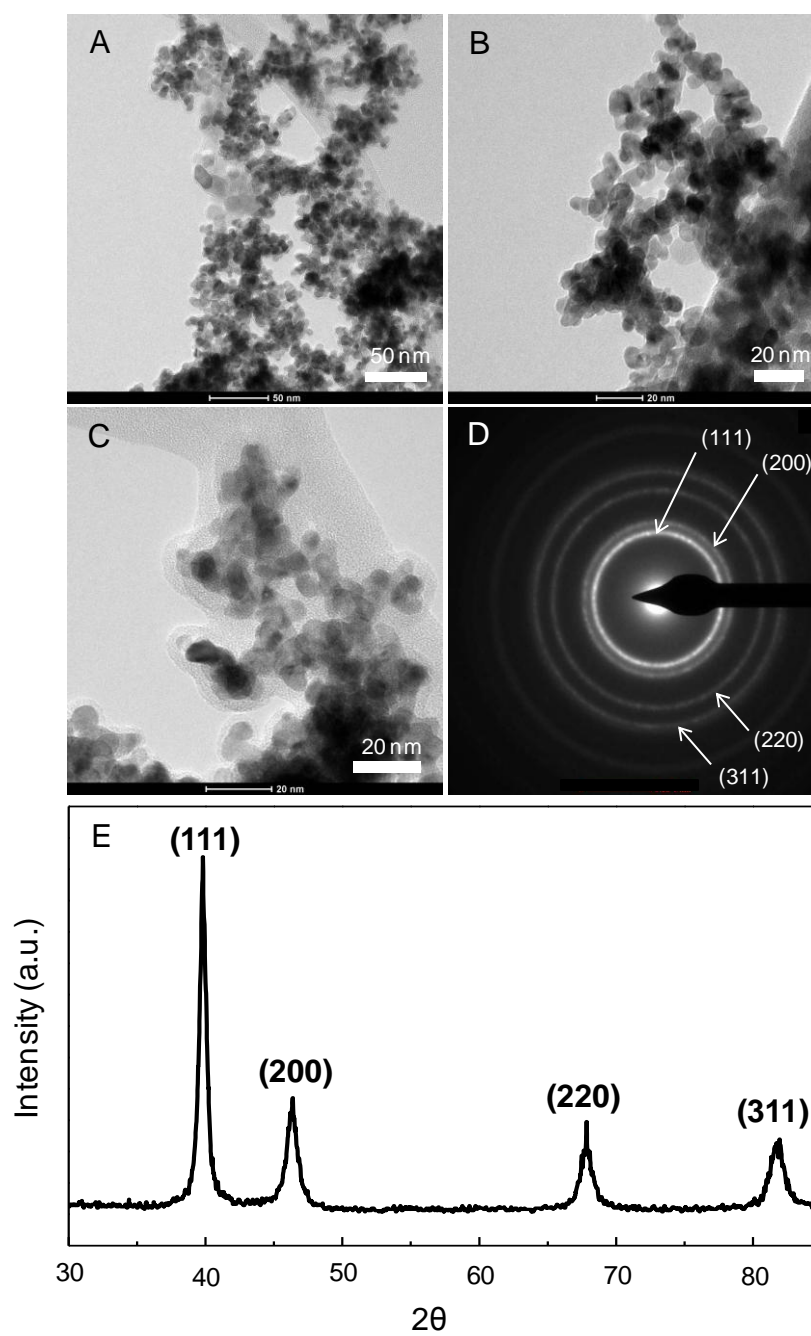


Figure 4.6 (A-C) TEM images, (D) electron diffraction pattern, and (E) XRD pattern of PdNPs synthesized by using acidic then alkaline-treated sucrose as a reducing agent.

#### 4.1.4 TEM images and crystal structure of palladium nanoparticles

The TEM images (Figure 4.6A-4.6C) confirm the aggregation of PdNPs synthesized by using acidic then alkaline-treated sucrose as a reducing agent and also the existence of sucrose covered on the particles (Figure 4.6C). However, the intrinsic size of the particles, which is around 10 nm, is revealed. The corresponding electron diffraction pattern reveals diffused rings assigned to (111), (200), (220), and (311) lattice planes corresponding to the face-centered cubic (fcc) crystal [34]. The XRD pattern with diffraction peaks ( $2\theta$ ) of  $39.8^\circ$ ,  $46.4^\circ$ ,  $67.8^\circ$ , and  $82.0^\circ$  confirms the fcc crystal structure [35, 36].

#### 4.1.5 Degradation of sucrose under acidic condition

Unlike most disaccharides, sucrose is a non-reducing sugar because of the formation of glycosidic bond between the reducing ends of both glucose and fructose. However, it can be converted into a reducing sugar by treating with acidic and alkaline solution. By treating with acidic solution, the glycosidic oxygen atom of sucrose is protonated and followed by heterolysis which glycosidic bond is broken down to form the two monosaccharides with one monosaccharide in the form of a cyclic oxocarbenium ion [37]. However, glucose or fructose carbonium ion can react with water to form D-glucose or D-fructose and regenerate the  $H^+$ . The schematic diagram of sucrose degradation under acidic condition is presented in Figure 4.7.

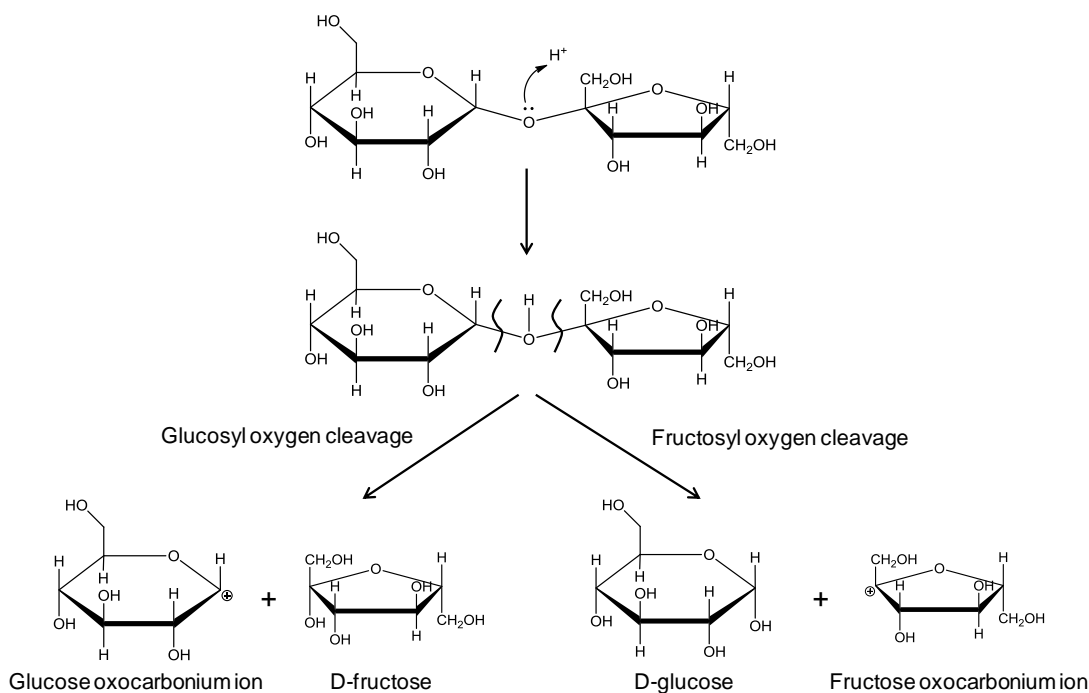


Figure 4.7 The mechanism of sucrose degradation under acidic condition.

#### 4.1.6 Degradation of monosaccharide under alkaline condition

Even sucrose was acidic-degraded to yield D-glucose and D-fructose which are both reducing sugar, the further degradation of these monosaccharide was conducted to generate smaller organic molecules with a higher reducing efficiency. Although D-glucose and D-fructose could undergo acidic degradation to yield smaller organic molecules nevertheless, the reaction is extremely slow. Alternatively, alkaline degradation could be better applied to degrade D-glucose and D-fructose. The alkaline degradation of monosaccharide is initiated by the reversible reaction which monosaccharide is rearranged via mutarotation and isomerization into enediol anion intermediate (Figure 4.8). This reaction is also known as the Lobry de Bruyn Alberda van Ekenstein rearrangement [37]. The generated enediol anion intermediate might be further degraded through non-reversible reactions.

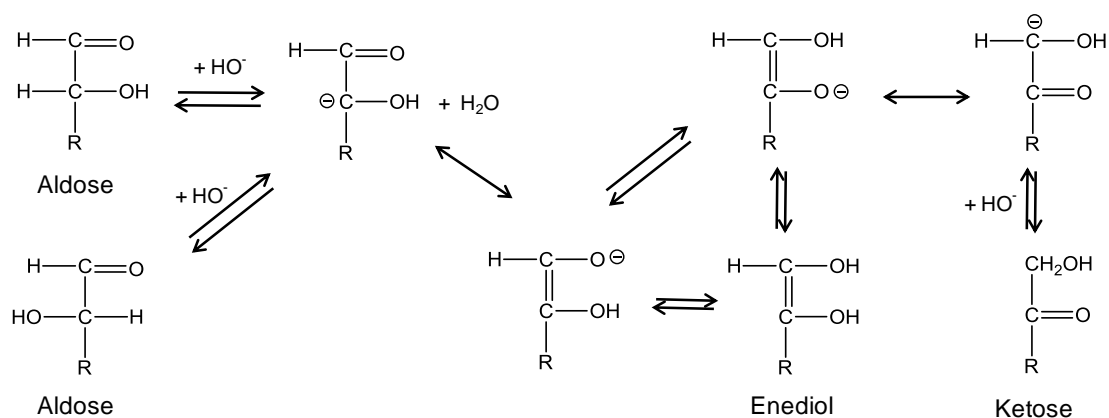


Figure 4.8 The mechanism of mutarotation and isomerization of monosaccharide to generate enediol anion intermediate.

The non-reversible degradation reactions can be described by five reaction types (Figure 4.9) which are  $\beta$ -elimination, benzilic acid rearrangement,  $\alpha$ -dicarbonyl cleavage, aldol condensation, and retro-aldol condensation [37]. These degradation reactions lead to the scission C-C bond and result in lower molecular weight organic acid products. These products are expected to be the reducing agents for the reduction of  $\text{PdCl}_4^{2-}$  to PdNPs. A simplified reaction scheme with the obtained products is shown in Figure 4.10.

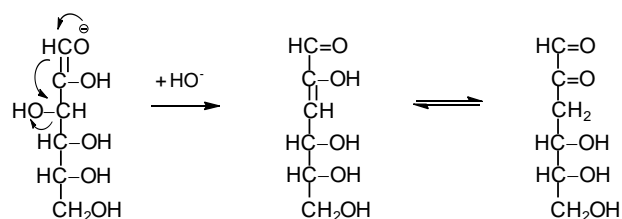
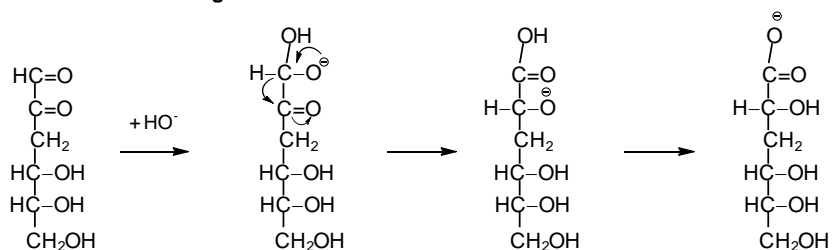
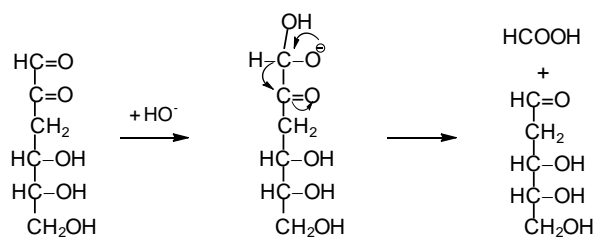
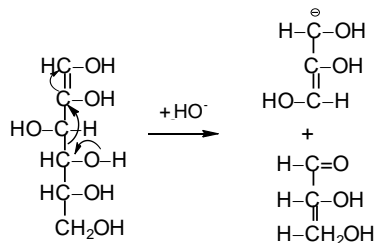
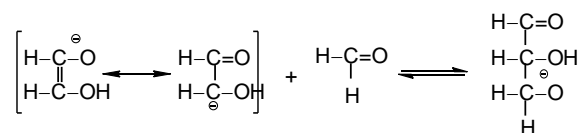
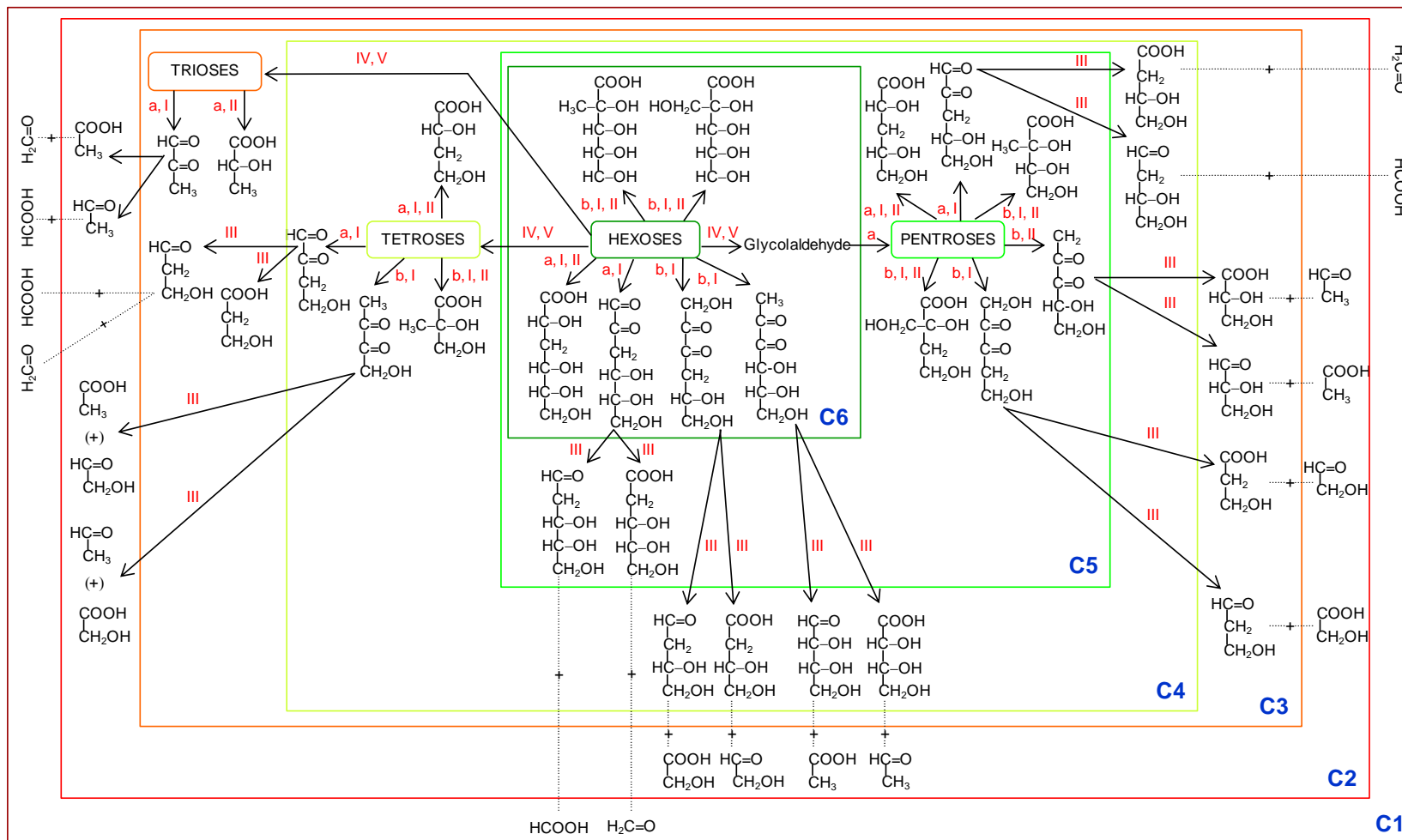
**I :  $\beta$ -elimination****II : benzilic acid rearrangement****III :  $\alpha$ -dicarbonyl cleavage****IV : retro-aldolization****V : aldolization**

Figure 4.9 The mechanism of monosaccharides degradation under alkaline condition.



a: 1,2-enediol, b: 2,3-enediol, I: β-elimination, II: benzilic and rearrangement, III: α-dicarbonyl cleavage, IV: retro-aldolization, V: aldolization

Figure 4.10 A simplified reaction scheme of monosaccharides degradation under alkaline condition [38].

#### 4.1.7 Investigation of sucrose degradation under acidic and alkaline conditions by ATR FT-IR spectroscopy

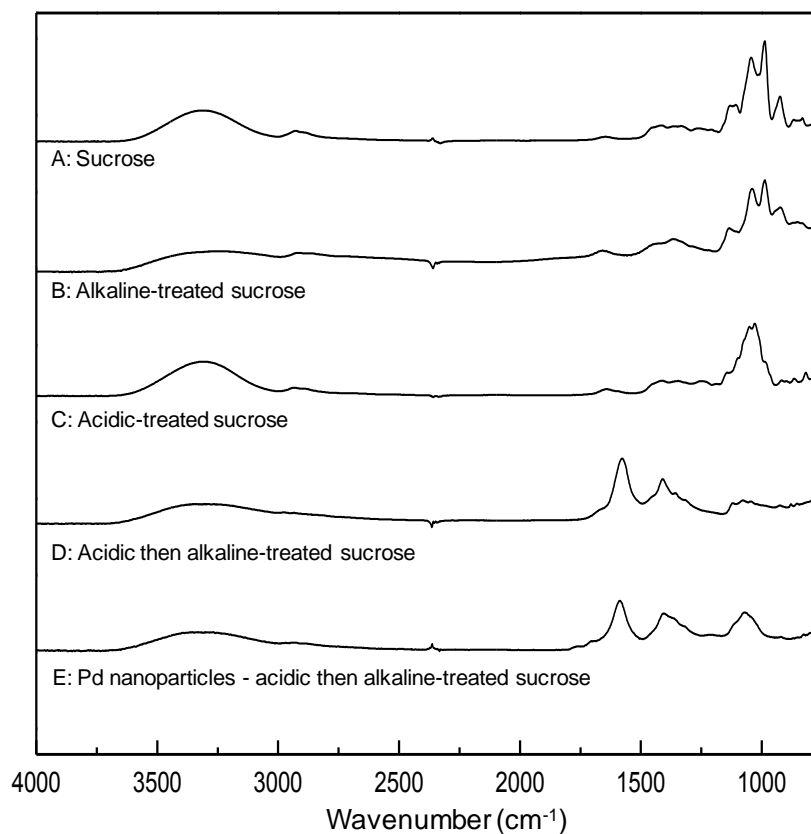


Figure 4.11 ATR FT-IR spectra of (A) sucrose, (B) alkaline-treated sucrose, (C) acidic-treated sucrose, (D) acidic then alkaline-treated sucrose, and (E) PdNPs synthesized by using acidic then alkaline-treated sucrose as reducing agent.

The ATR FT-IR spectra demonstrate functional group transformations of sucrose after acidic and alkaline treatments (Figure 4.11). Original sucrose has broad band from 3700 to 3000 cm<sup>-1</sup> due to the OH stretch vibration ( $\nu_{\text{OH}}$ ), band in the 2700 to 3000 cm<sup>-1</sup> region for the C-H stretching modes, intense bands in the 1000 cm<sup>-1</sup> region for the C-O and C-C stretch vibrations, and a broad band around 1400 cm<sup>-1</sup> for the C-C-H and C-O-H deformation modes [39]. After the acidic treatment, there is a

change of the spectral feature in the  $1000\text{ cm}^{-1}$  region due to the breaking down of glycosidic bond linkage between glucose and fructose units. On the other hand, there is no significant change of the spectrum after the alkaline treatment. Thereafter, the acidic treated sucrose was further treated with alkaline solution. The spectrum was significantly changed. There are the appearance of the absorption band around  $1580$  and  $1410\text{ cm}^{-1}$  which correspond to the asymmetric ( $\nu_{\text{as}}(\text{COO}^-)$ ) and symmetric ( $\nu_{\text{s}}(\text{COO}^-)$ ) carbonyl bonds of the acid salts, respectively [40]. These indicate that sucrose was converted to organic compound with the acid-functional group by the alkaline treatment, particularly when sucrose was pre-treated with acid solution. The generated acid-functional group was believed to be the reducing end for the reduction of  $\text{PdCl}_4^{2-}$  to Pd metal. Moreover, the spectrum of synthesized PdNPs was collected and the result shows that there are three absorption bands of the asymmetric ( $\nu_{\text{as}}(\text{COO}^-)$ ) and symmetric ( $\nu_{\text{s}}(\text{COO}^-)$ ) carbonyl bonds of the acid salts, C-O and C-C stretch vibrations, and OH stretch vibration ( $\nu_{\text{OH}}$ ). These findings confirm the existence of organic acid compound binding on the surface of PdNPs [33].

## 4.2 Sucrose induced formation of palladium film at air-water interface

### 4.2.1 Formation of palladium film at air-water interface

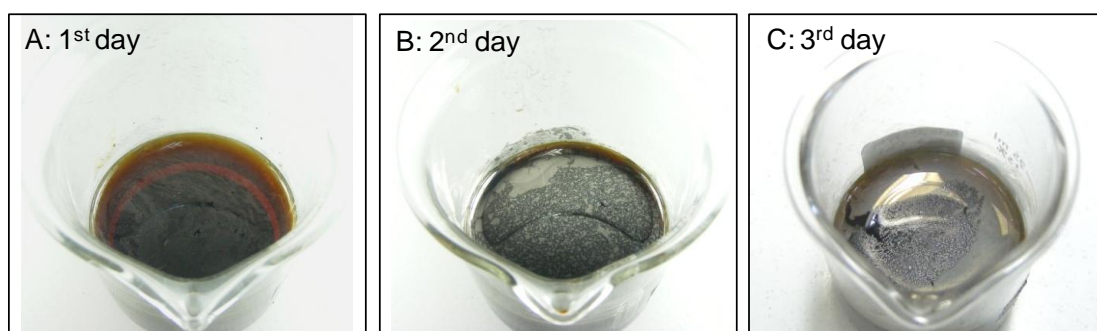


Figure 4.12 Optical images depicting the formation of Pd film at air-water interface.

Optical images (Figure 4.12) show that a shiny palladium film gradually formed at air-water interface and became more apparent within two days after the reaction. The morphology of the film was investigated by SEM and the results reveal that the film was composed of nano-sized Pd particles inter-connected with each other



(Figure 4.13A and 4.13B). The average size of each particle is 50 nm. The corresponding energy dispersive X-ray (EDX) spectrum (Figure 4.13C) indicates that Pd film is dominantly composed of Pd metal. The carbon (C) element in the EDX-spectrum is originated from the employed carbon tape substrate.

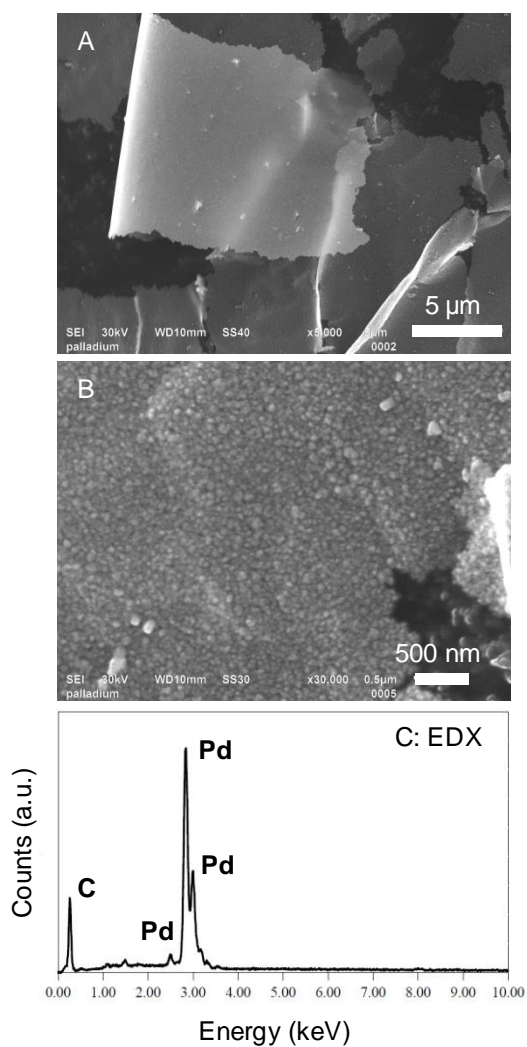


Figure 4.13 SEM micrographs of Pd film (A) lower and (B) higher magnifications, and (C) EDX spectrum.

#### 4.2.2 The time-dependent investigating formation of palladium film at air-water interface

The time-dependent investigation of Pd film formation reveals that the Pd film evolves from the self-assembly of spherical PdNPs with the particle size in the

range of 50 to 100 nm. The nanoparticles inter-connected together to form aggregates with porous structures in the first two days after reaction (Figure 4.14A and 4.14B). After that, the nanoparticle aggregates became less porous (Figure 4.14C) as the additional nanoparticles filled in the space between aggregates. Finally, the PdNPs aggregates transformed into Pd film with no porosity within 5 days (Figure 4.14D). Moreover, there was a change of the film morphology within 8 and 16 days after reaction. The PdNPs, which connected together, changed from spherical shape (Figure 4.14D) to a shape with more edge and corner (Figure 4.14E and 4.14F). The particle size also increased from 100 (Figure 4.14D) nm to 300 (Figure 4.14E) and 400 (Figure 4.14F) nm, respectively.

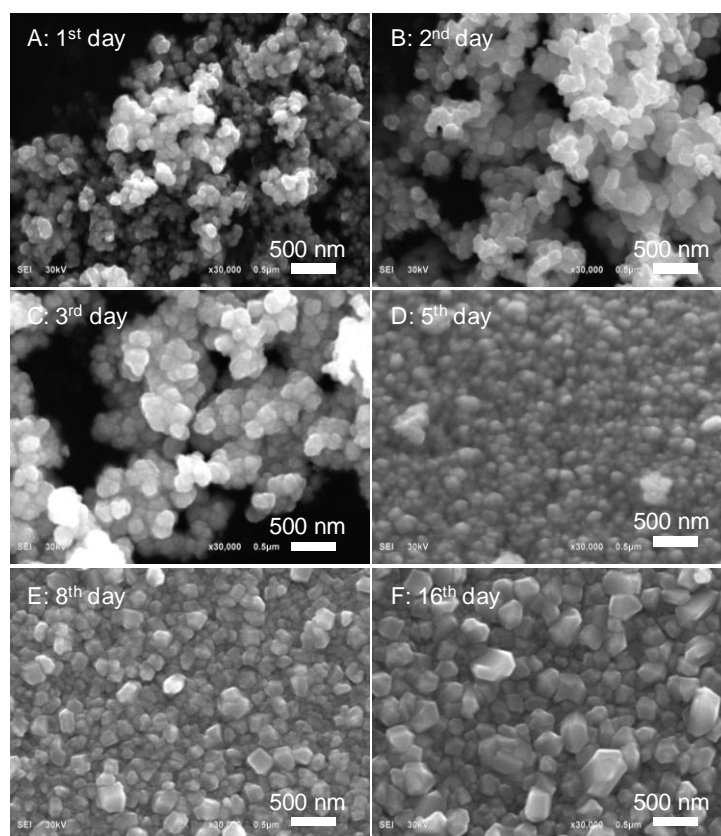


Figure 4.14 (A-F) SEM micrographs revealing evolution of Pd film formation at air-water interface.

The UV-vis spectra of supernatant were collected to study the formation of Pd film. As mentioned in the experimental section that the formation of Pd film at

air-water interface occurred only when a high concentration (5,000 ppm) of  $\text{PdCl}_4^{2-}$  was employed for the synthesis of PdNPs by using acidic then alkaline-treated sucrose as a reducing agent. Therefore, the major factor for the formation of Pd film is the concentration of used  $\text{PdCl}_4^{2-}$ . As found that Pd film evolved from the self-assembly of PdNPs. However, the PdNPs was precipitated down after finished the reaction as there was no UV-vis absorption in the 300 nm to 700 nm region. Therefore, PdNPs which assembled to palladium film should come from the reduction of  $\text{PdCl}_4^{2-}$  which remained in the solution. The time-dependent investigation by UV-vis spectroscopy could be used to prove this assumption. The decrease of UV-vis absorption peak at 420 nm, which is the characteristic of  $\text{PdCl}_4^{2-}$  [41], indicates the consumption of  $\text{PdCl}_4^{2-}$  (Figure 4.15). Although the reaction was finished by stopping heating and stirring, the reduction of  $\text{PdCl}_4^{2-}$  still occurred under ambient condition.  $\text{PdCl}_4^{2-}$  was reduced to PdNPs which then migrated to the air-water interface by the Brownian motion. The particles entrapped by the surface tension of air-water interface and aggregated together into film [42, 43]. Moreover, the nanoparticles, which aggregated into film, also acted as nucleation sites for the further growth resulted into a more complex film surface.

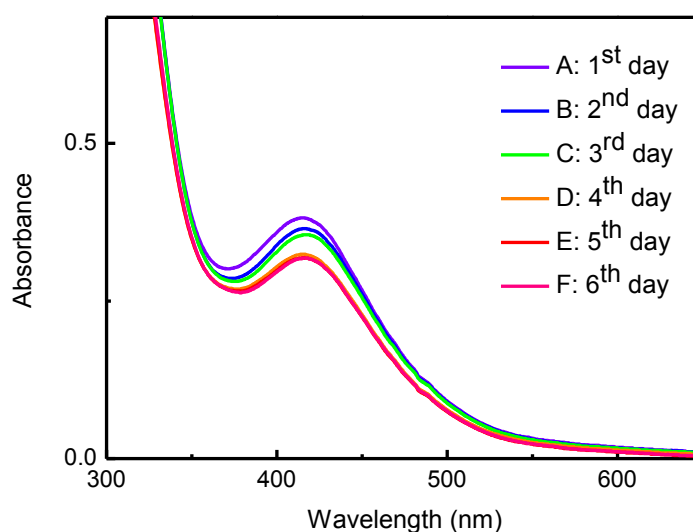


Figure 4.15 UV-vis spectra revealing the decrease of  $\text{PdCl}_4^{2-}$  absorbance in 6 days after stopping the reaction.

### 4.2.3 The crystal structure of palladium film

The XRD pattern (Figure 4.16) of Pd film exhibits diffraction peak ( $2\theta$ ) at  $40.1^\circ$ ,  $46.6^\circ$ ,  $68.1^\circ$ , and  $82.1^\circ$  assigned to (111), (200), (220), and (311) lattice planes, respectively. This XRD result informs the fcc crystal structure [35, 36].

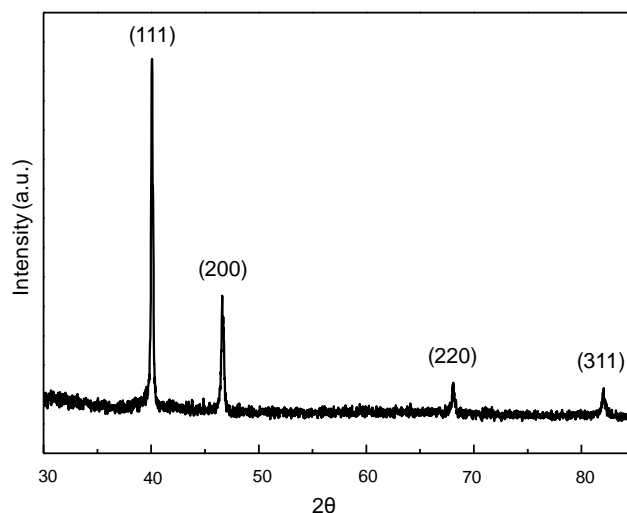


Figure 4.16 XRD pattern of Pd film.

## 4.3 Flowerlike palladium microstructures synthesized by using hydrogen peroxide as a sole reducing agent

### 4.3.1 Formation of flowerlike palladium microstructures

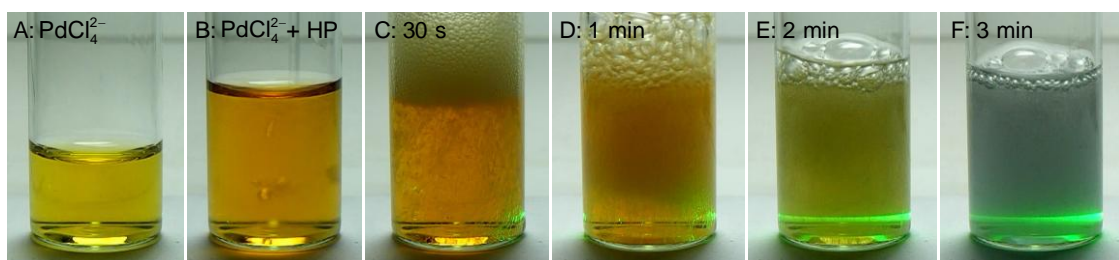


Figure 4.17 Optical images depicting the evolution of FPd $\mu$ STs synthesizing by mixing 5.64 mM PdCl $_4^{2-}$  solution with 30% HP. The particle evolution was monitored through the scattering of a green laser pointer.

As shown in Figure 4.17, FPd $\mu$ STs were simply produced by mixing a yellow solution of PdCl $_4^{2-}$  and a colorless HP. The mixture immediately turned yellow-orange. A burst of large number of small bubbles occurred within 30 s after mixing. After the collapse of the bubbles, the solution gradually turned black indicating a formation of Pd-black particles. During the course of reaction, the development of particles was monitored via a light scattering of a green laser pointer. An onset of the Tyndall's effect suggests that particles formed after the collapse of the bubbles (Figure 4.17E). SEM micrographs revealed uniform and well-separated FPd $\mu$ STs with an approximate particle size of 2  $\mu$ m (Figure 4.18). The corresponding energy dispersive X-ray (EDX) spectrum (Figure 4.18C) indicated that FPd $\mu$ STs were dominantly composed of Pd metal. The carbon (C) element in the EDX-spectrum originated from the employed carbon tape substrate.

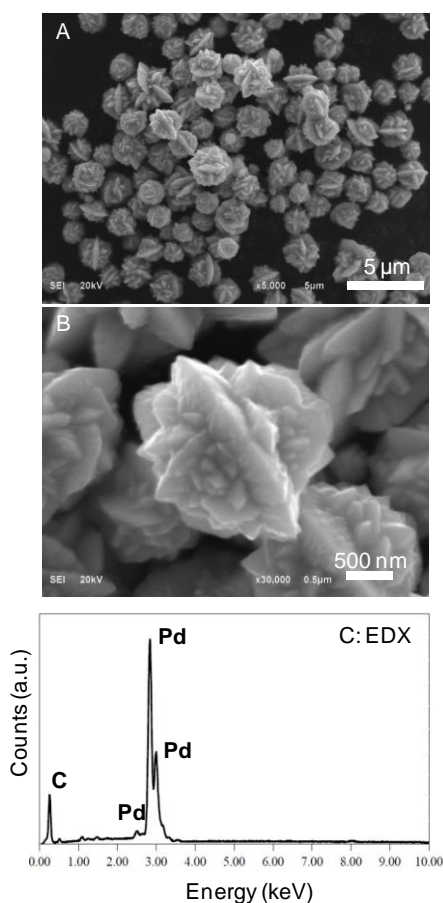
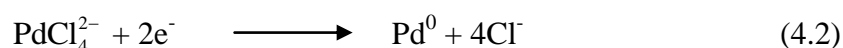
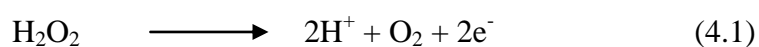


Figure 4.18 SEM micrographs of FPd $\mu$ STs at (A) lower and (B) higher magnifications and (C) EDX spectrum.

Although HP is known as a powerful oxidizing agent, it can function as a reducing agent under an acidic condition [44] (equations 4.1 and 4.2). The formation of FPd $\mu$ STs is due to the reduction of PdCl $_4^{2-}$  by HP into PdNPs. Since there was no surfactant or capping agent employed under an excess HP environment, the PdNPs undergo self-seeding for aggregation and epitaxial growth into FPd $\mu$ STs. A rapid reduction and a concomitantly structural transformation were realized by the sudden burst of small O $_2$  bubbles.



#### 4.3.2 Effect from the concentration of PdCl $_4^{2-}$ and hydrogen peroxide

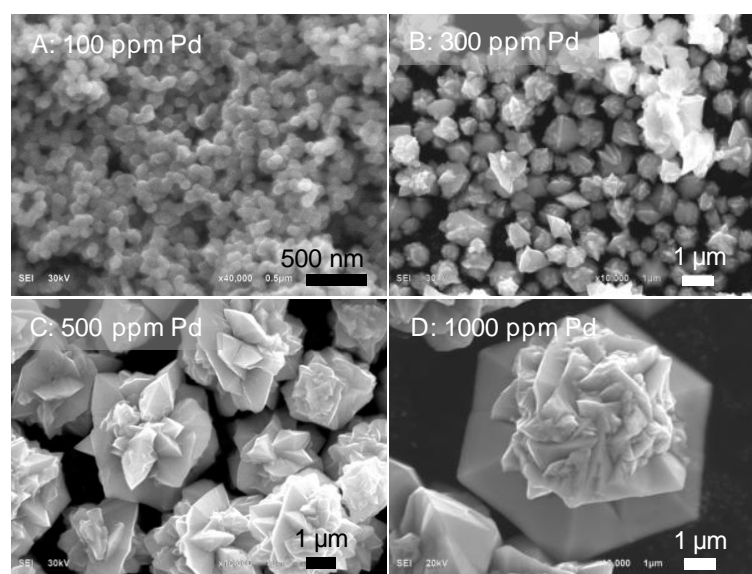


Figure 4.19 SEM micrographs of PdNPs and FPd $\mu$ STs synthesized using 15% HP with PdCl $_4^{2-}$  concentration of (A) 100, (B) 300, (C) 500, and (D) 1000 ppm.

According to our study, adjusting concentrations of PdCl $_4^{2-}$  and HP could control the particle morphology. Increasing the concentration of PdCl $_4^{2-}$  from 300 to 500 and 1000 ppm (at a constant HP concentration of 15%) increased the size of

FPd $\mu$ STs from 1, to 3 and 5  $\mu$ m, respectively. Moreover, complexity of the obtained FPd $\mu$ STs was also increased (Figure 4.19). This could be explained by a larger metal supply and a greater rate of crystal growth as the concentration of PdCl $_4^{2-}$  increased. It should be noted that at a low PdCl $_4^{2-}$  concentration of 100 ppm, the metal ion supply [18, 34] was too low to induce the formation of the flowerlike microstructure. As a result, spherical PdNPs with an average particle size of 100 nm were obtained (Figure 4.19A).

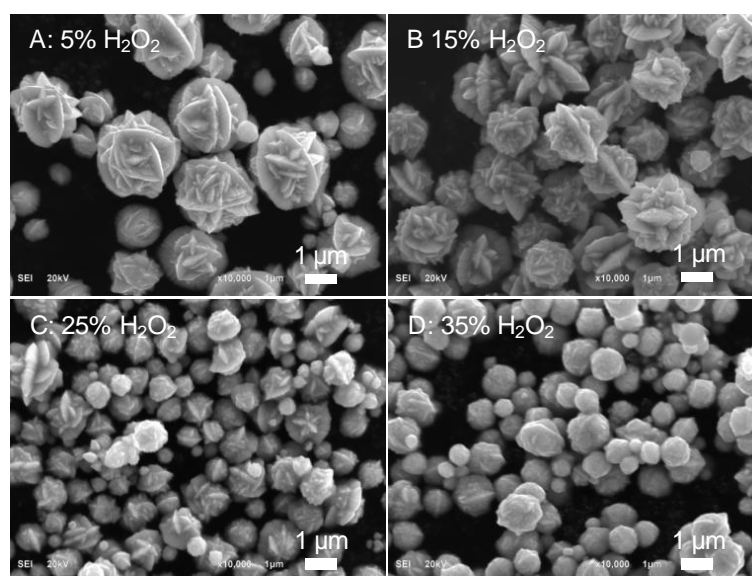


Figure 4.20 SEM micrographs of FPd $\mu$ STs synthesized using 400 ppm PdCl $_4^{2-}$  with HP concentration of (A) 5, (B) 15, (C) 25, and (D) 35 %.

On the other hand, increasing the concentration of HP from 5 to 35% (at a constant PdCl $_4^{2-}$  concentration 400 ppm) reduced the particle size of FPd $\mu$ STs from 5  $\mu$ m to 500 nm as well as diminished the complexity of the flowerlike structures (Figure 4.20). The FPd $\mu$ STs synthesized by 5% HP had an average particle size of 3  $\mu$ m. When the concentration of HP was increased to 15, 25, and 35%, the particle size reduced to 2, 1, and 1  $\mu$ m, respectively, with noticeable reduced complexity. It should be noted that the complexity of the FPd $\mu$ STs synthesized with 35% HP was diminished to almost quasi-spherical particles with smooth surfaces. The decrease of

particle size and complexity were due to a greater nucleation rate at high HP concentration [23, 45, and 46].

#### 4.3.3 The time-dependent shape evolution of flowerlike palladium microstructures

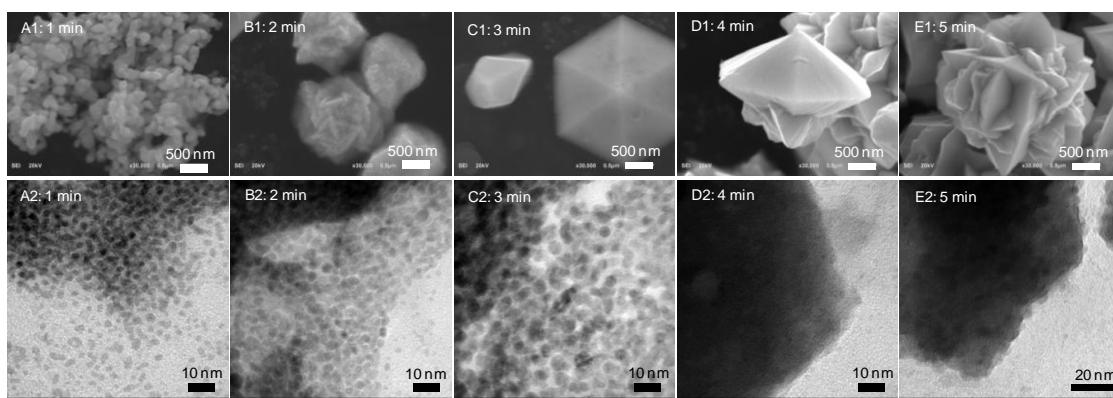


Figure 4.21 (A - E) SEM and (F - J) TEM images revealing evolution of FPd $\mu$ STs and the formation of FPd $\mu$ STs from PdNPs.

The time-dependent investigation of FPd $\mu$ STs formation reveals that the FPd $\mu$ STs evolved from the assembly of small spherical PdNPs with an average particle size of 3 nm, as investigated by SEM and TEM (Figure 4.21). Initially, the nano-sized Pd particles were generated via nucleation and growth of Pd atoms from the reduction of PdCl<sub>4</sub><sup>2-</sup> by HP. Since there was no stabilizer or capping agent employed, the primary PdNPs self-aggregated into secondary particles (Figure 4.21 A1) because of the lack of stabilizing property. The secondary particles were further growth into Pd $\mu$ STs with the hexagonal bi-pyramid shape (Figure 4.21 B1 and 4.21 C1) and finally growth into FPd $\mu$ STs (Figure 4.21 D1 and 4.21 E1). Furthermore, TEM images show the intrinsic particle size (3 nm) of primary PdNPs (Figure 4.21 A2) and also reveal the increase of primary particle size from 3 to 5 (Figure 4.21 B2) and to 7 (Figure 4.21 C2) nm, respectively. TEM analysis also confirms the further growth of secondary particles (aggregated primary particles) into Pd $\mu$ STs with the hexagonal bi-pyramid shape (Figure 4.21 D2) and FPd $\mu$ STs (Figure 4.21 E2). From



this investigation, a possible formation mechanism of FPd $\mu$ STs was proposed as shown in Figure 4.22. It is clear that how the primary PdNPs were produced and then aggregated into secondary PdNPs. However, it is still doubtful that how the secondary PdNPs are growth into Pd $\mu$ STs with the hexagonal bi-pyramid shape and finally growth into FPd $\mu$ STs. As mentioned previously that there were no stabilizer or capping agent employed to dictate the growth of PdNPs. In this case, one possible explanation is regarding the strain relief which aggregated nanoparticles further growth by filling the space of the aggregated structure [30, 47]. This is also known as a surface-energy minimization process. The evidence that supports this explanation is the SEM micrographs of PdNPs synthesized at low concentration of PdCl $_4^{2-}$  (100 ppm). As presented previously that spherical PdNPs with an average particle size of 100 nm were obtained (Figure 4.19A) because the metal ion supply was too low to induce the formation of the flowerlike microstructures. However, some minor microstructures were produced besides spherical shape. These microstructures are the uncompleted growth of hexagonal bi-pyramid shape. The amount of Pd atom addition was not enough to fulfill the space of an aggregated structure. Thus, the groves remained on the crystal facets. Examples of some uncompleted growth microstructures, which could be used to explain the strain relief growth of microstructures, were shown in SEM micrographs (Figure 4.23). The microstructures with deep groves (Figure 4.23A) suppose to be the structure in the early stage of growth. In the middle stage of growth, the groves become shallower and the particle size increased from 2 to 3  $\mu$ m (Figure 4.23B). The microstructures in the last stage of growth (Figure 4.23C) have the shape which is closed to the hexagonal bi-pyramid shape. In addition, Figure 4.23D confirms the evolution of microstructures by aggregation and then growth of spherical PdNPs. Although it is clear that FPd $\mu$ STs are produced by the aggregation of PdNPs and then growth by the strain relief, further investigation should be made in order to gain insight understanding about the growth mechanism.

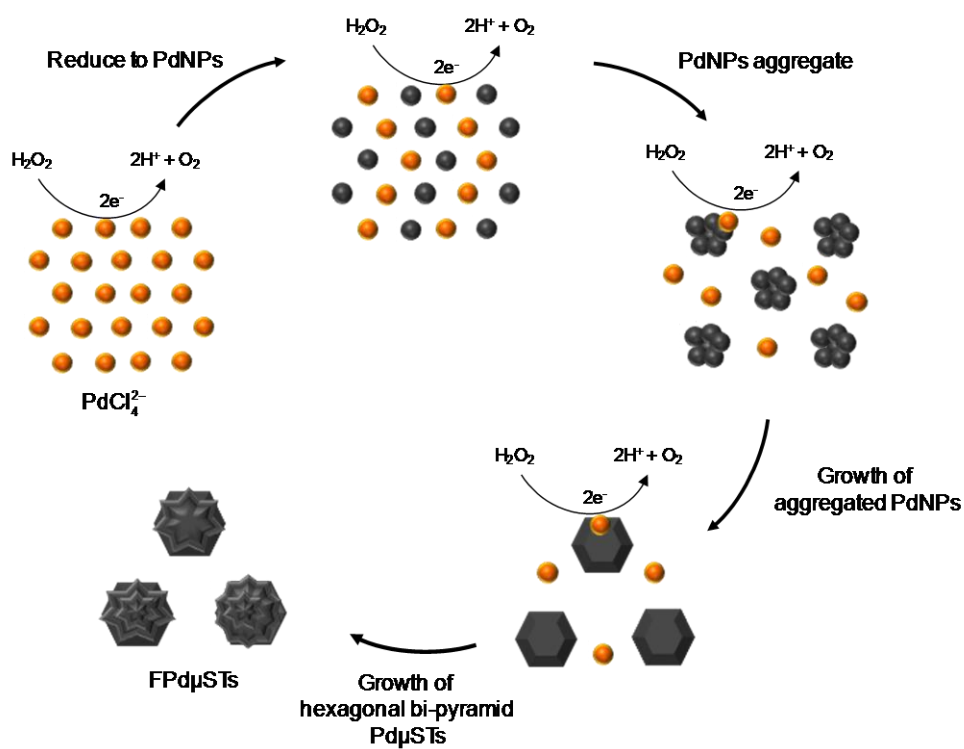


Figure 4.22 The schematic diagram illustrates the formation mechanism of FPd $\mu$ STs.

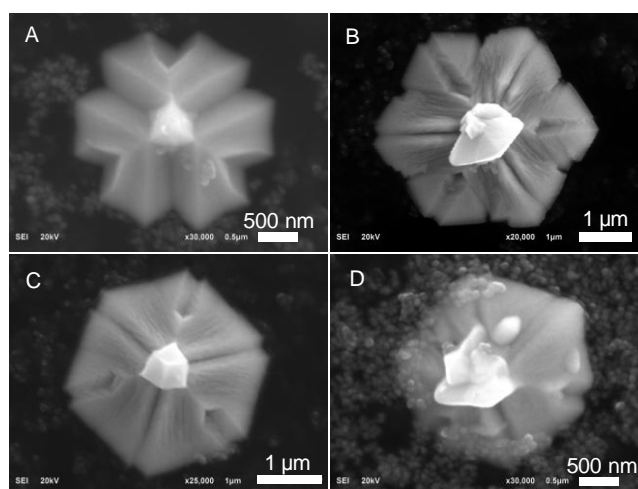


Figure 4.23 (A - D) SEM micrographs of Pd $\mu$ STs (minor structures) synthesized by using 15% HP and 100 ppm of PdCl<sub>4</sub><sup>2-</sup>.

#### 4.3.4 The crystal structure of flowerlike palladium microstructures

The TEM image (Figure 4.24A) shows FPd $\mu$ STs with the size approximately 1.5  $\mu\text{m}$ . The corresponding electron diffraction pattern (Figure 4.24B) reveals diffused rings assigned to (111), (200), (220), and (311) lattice planes corresponding to the face-centered cubic (fcc) crystal [34]. The XRD pattern (Figure 4.24C) with diffraction peaks ( $2\theta$ ) of 40.0°, 46.6°, 68.0°, and 82.1° confirms the fcc crystal structure [35, 36].

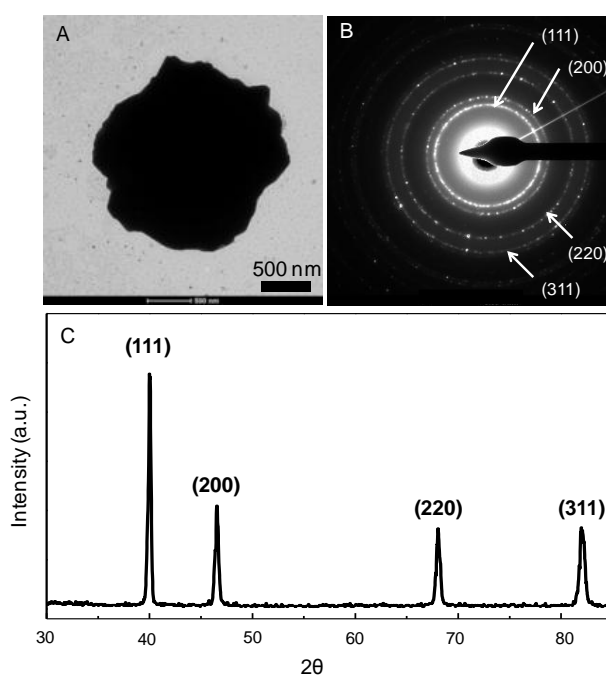


Figure 4.24 (A) TEM image, (B) electron diffraction pattern, and (C) XRD pattern of FPd $\mu$ STs.

## CHAPTER V

### CONCLUSIONS

A novel and environmental-friendly approach for the synthesis of high-concentration PdNPs was developed. Sucrose was used as a reducing agent for the reduction of  $\text{PdCl}_4^{2-}$  to PdNPs. Alkaline treatment is an important factor for the generation of sucrose reducing property especially when sucrose was pre-treated under acidic condition. Spherical PdNPs with particle size of 10 to 100 nm were obtained. This approach can be scaled-up for the production of high-concentration PdNPs for industrial use with a highly competitive price.

Pd film at air-water interface was prepared by self-assembly of PdNPs synthesized by using acidic then alkaline-treated sucrose as reducing agent. The time-dependent investigation of the Pd film formation reveals that the Pd film evolves from the self-assembly of spherical PdNPs with the particle size in the range of 50 to 100 nm.  $\text{PdCl}_4^{2-}$  was reduced to PdNPs which then migrated to the air-water interface by the Brownian motion. The particles entrapped by the surface tension of air-water interface and aggregated together into film. Moreover, the nanoparticles, which aggregated into film, also acted as nucleation sites for the further growth resulted into a more complex film surface. The obtained Pd film has a potential to be applied as sensor and surface-enhanced Raman substrate.

FPd $\mu$ STs were synthesized by a novel and environmental-friendly approach. Hydrogen peroxide was used as a reducing agent for the reduction of  $\text{PdCl}_4^{2-}$ . FPd $\mu$ STs with particle size in the range of 1 - 5  $\mu\text{m}$  were obtained. The time-dependent investigation the FPd $\mu$ STs formation reveals that the FPd $\mu$ STs evolved from the assembly of small spherical PdNPs with an average particle size of 3 nm. The nano-sized Pd particles were generated via nucleation and growth of Pd atoms from the reduction of  $\text{PdCl}_4^{2-}$ . The primary particles self-aggregated into secondary particles because of the lack of stabilizing property. The secondary particles were

further growth into Pd $\mu$ STs with the hexagonal bi-pyramid shape and finally growth into FPd $\mu$ STs. The obtained microstructures are expected to express high catalytic activity since their surfaces were naked.

In conclusion, this research is fulfilled the research objective.

## REFERENCES

- [1] Mongillo, J. Nanotechnology 101. Westport, CT: Green Wood Press, 2007.
- [2] Li, D. Synthesis of metal nanoparticles by microwave-assisted solvothermal technique. Doctoral dissertation, Intercollege Graduate Program in Materials, Graduate School, Pennsylvania State University, 2005.
- [3] Nassos, S. Development of catalytic nanomaterials for three industrial processes. Doctoral dissertation, Department of Applied Surface Chemistry, Chemical and Biological Engineering, Goteborg University of Technology, 2007.
- [4] Hou, W. Quasi-homogeneous gold and bimetallic nanoparticle catalysts. Master's Thesis, College of Graduate Studies and Research, Department of Chemistry, University of Saskatchewan, 2008.
- [5] Albeniz, A.C. and Espinet, P. Palladium: Inorganic & Coordination Chemistry. Encyclopedia of Inorganic Chemistry (2005).
- [6] Miyaura, N. and Suzuki, A. Palladium-catalyzed cross-coupling reactions of organoboron compounds. Chem. Rev. 95 (1995): 2457-2483.
- [7] Pillai, U.R. and Demessie, E.S. Phenanthroline-stabilized palladium nanoparticles in polyethylene glycol—an active and recyclable catalyst system for the selective hydrogenation of olefins using molecular hydrogen. J. Mol. Catal. A: Chem. 222 (2004): 153-158.
- [8] Teschner, D., et al. The roles of subsurface carbon and hydrogen in palladium-catalyzed alkyne hydrogenation. Science 320 (2008): 86-89.
- [9] Liu, Y., Hu, J., Kong, Q., and Feng, X. Shaped-controlled synthesis and application in surface-enhanced Raman scattering of novel palladium nanoparticles. Mater. Lett. 64 (2009): 422-424.
- [10] Niu, W., Zhang, L., and Xu, G. Shape-controlled synthesis of single-crystalline palladium nanocrystals. ACS Nano 4 (2010): 1987-1996.
- [11] Rice, C., Ha, S., Masel, R.I., and Wieckowski, A. Catalysts for direct formic acid fuel cells. J. Power Sources 15 (2003): 229-235.

- [12] Umicore. Catalytic converter. [Online]. 2012. Available from: <http://www.auto-catalyst-recycling.umicore.com/catalyticConverter/> [2012, March 15]
- [13] Global Energy Network Institute. Articles on H2-Fuel cell Vehicles [Online]. 2012. Available from: <http://www.geni.org/globalenergy/library/articles-renewable-energy-transmission/h2-fuel-cell.shtml> [2012, March 15]
- [14] Naka, K., Itoh, H., and Chujo, Y. Self-organization of spherical aggregates of palladium nanoparticles with a cubic silsesquioxane. Nano Lett. 2 (2002): 1183-1186.
- [15] Xuing, Y., and Xia, Y. Shape-controlled synthesis of metal nanostructures: the case of palladium. Adv. Mater. 19 (2007): 3385-3391.
- [16] Chang, G., Oyama, M., and Hirao, K. Facile synthesis of monodisperse palladium nanocubes and the characteristics of self-assembly. Acta Mater. 55 (2007): 3453-3456.
- [17] Toshima, N., and Yonezawa, T. Bimetallic nanoparticles—novel materials for chemical and physical applications. New J. Chem. (1998): 1179-1201.
- [18] Papp, S., and Dekany, I. Nucleation and growth of palladium nanoparticles stabilized by polymers and layer silicates. Colloid. Polym. Sci. 284 (2006): 1049-1056.
- [19] Lipson, M. Controlling light with light. [Online]. 2004. Available from: <http://people.ece.cornell.edu/lipson/nature/fabrication.htm> [2012, March 15]
- [20] Lee, M. Mineralogy at the nanoscale using the focused ion beam (FIB) technique. [Online]. 2012. Available from: <http://web2.ges.gla.ac.uk/~mlee/FIBtec.htm> [2012, March 15]
- [21] He, F., Liu, J., Roberts, C.B., and Zhao, D. One-step “green” synthesis of pd nanoparticles of controlled size and their catalytic activity for trichloroethene hydrodechlorination. Ind. Eng. Chem. Res. 48 (2009): 6550-6557.
- [22] Jackson, E., and Pantony, D.A. Investigations in platinum metal group electrochemistry: II the Pd(II)-Pd<sup>0</sup> reduction. J. Appl. Electrochem. 1 (1971): 283-291.

- [23] Teranishi, T., and Miyake, M. Size control of palladium nanoparticles and their crystal structures. Chem. Mater. 10 (1998): 594-600.
- [24] Yonezawa, T., Imamura, K., and Kimizuka, N. Direct preparation and size control of palladium nanoparticle hydrosols by water-soluble isocyanide ligands. Langmuir 17 (2001): 4701-4703.
- [25] Kim, S.W., Park, J., Chung, Y., Hwang, S., and Hyeon, T. Synthesis of monodisperse palladium nanoparticles. Nano Lett. 3 (2003): 1298-1291.
- [26] Dahl, J.A., Maddux, B.L.S., and Hutchison, J.E. Toward greener nanosynthesis. Chem. Rev. 107 (2007): 2228-2269.
- [27] Panigrahi, S., Kundu, S., Ghosh, S.K., Nath, S., and Pal, T. General method of synthesis for metal nanoparticles. J. Nanopart. Res. 6 (2004): 411-414.
- [28] Nadagouda, M.N., and Varma, R.S. Green synthesis of Ag and Pd nanospheres, nanowires, and nanorods using vitamin B<sub>2</sub>: catalytic polymerisation of aniline and pyrrole. J. Nanomater. (2007): 2-9.
- [29] Yang, X., et al. Green synthesis of palladium nanoparticles using broth of cinnamomum camphora leaf. J. Nanopart. Res. 12 (2009): 1589-1598.
- [30] Xia, Y., Xiong, Y., Lim, B., and Skrabalak, S.E. Shape-controlled synthesis of metal nanocrystals: simple chemistry meets complex physics. Angew. Chem. Int. Ed. 48 (2009): 60-103.
- [31] Aiken III, J.D., and Finke, R.G. A review of modern transition-metal nanoclusters: their synthesis, characterization, and applications in catalysis. J. Mol. Catal. A: Chem. 145 (1999): 1-44.
- [32] Krafft, T.E. Preparation of bis(acetonitrile) palladium dichloride. US patent 5681976 (1997).
- [33] Shin, Y., Bae, I., and Exarhos, G.J. "Green" approach for self-assembly of platinum nanoparticles into nanowires in aqueous glucose solutions. Colloids Surf., A 348 (2009): 191-195.
- [34] Ho, P., and Chi, K. Size-controlled synthesis of Pd nanoparticles from  $\beta$ -diketonato complexes of palladium. Nanotechnology 15 (2004): 1059-1064.



- [35] Bankar, A., Joshi, B., Kumar A.R., and Zinjarde, S. Banana peel extract mediated novel route for the synthesis of palladium nanoparticles. Mater. Lett. 64 (2010): 1951-1953.
- [36] Wang, W., Guan, H., Chen, T., Wu, D., and Zhang, G. Surface-assisted synthesis and characterization of Pd nanorods. Mater. Lett. 66 (2012): 332-334.
- [37] Horton, D. Advances in carbohydrate chemistry and biochemistry. 52. San Diego, CA: Academic Press, 1997.
- [38] Tongsakul, D. Platinum nanoparticles synthesized via green nanotechnology. Doctoral dissertation, Faculty of Science, Chulalongkorn University, 2011.
- [39] Max, J.J., and Chapados, C. Sucrose hydrates in aqueous solution by IR spectroscopy. J. Phys. Chem. A 105 (2001): 10681-10688.
- [40] Max, J.J., and Chapados, C. Infrared spectroscopy of aqueous carboxylic acids: comparison between different acids and their salts. J. Phys. Chem. A 108 (2004): 3324-3337.
- [41] Luo, C., Zhang, Y., and Wang, Y. Palladium nanoparticles in poly(ethyleneglycol): the efficient and recyclable catalyst for Heck reaction. J. Mol. Catal. A: Chem. 229 (2005): 7-12.
- [42] Hu, J., Zhao, B., Xu, W., Fan, Y., Li, B., and Ozaki, Y. Aggregation of silver particles trapped at an air-water interface for preparing new SERS active substrates. J. Phys. Chem. B 106 (2002): 6500-6506.
- [43] Wang, L., Sun, Y., Che, G., and Li, Z. Self-assembled silver nanoparticle films at an air-liquid interface and their applications in SERS and electrochemistry. Appl. Surf. Sci. 257 (2011): 7150-7155.
- [44] Bancroft, W.D., and Nelson, N.F. Oxidation and reduction with hydrogen peroxide. J. Phys. Chem. 3 (1935): 377-398.
- [45] Wang, C., Chen, D., and Huang, T. Synthesis of palladium nanoparticles in water-in-oil microemulsions. Colloids Surf., A 189 (2001): 145-154.
- [46] Hussain, S.T., Iqbal, M., and Mazhar, M. Size control synthesis of starch capped-gold nanoparticles. J. Nanopart. Res. 11 (2009): 1383-1391.
- [47] Tao, A.R., Habas, S., and Yang, P. Shape control of colloidal metal nanocrystals. Small 3 (2008): 310-325.

## VITAE

**Name:** Mr. Lunjakorn Amornkitbamrung

**Date of Birth:** October 6, 1986                      **Birth place:** Khonkaen, Thailand

**Address:** 123/189, Mitrapap Road, Mueang Khonkaen, 40002, Thailand

E-mail address: chevonton@hotmail.com

**Education:**

2008                      Bachelor of Science in Chemistry  
Chulalongkorn university, Thailand

2011                      Master of Science in Chemistry  
Chulalongkorn University, Thailand

**Awards:**

January 5-7, 2011	First Prize Student Oral Presentation in The 28 <sup>th</sup> Annual Conference of the Microscopy Society of Thailand, Thailand
March 10-11, 2011	Honorable Mention in The Science Forum 2011, Chulalongkorn University, Thailand
February 5-9, 2012	AMMS Bursary Winner in 10 <sup>th</sup> Asia-Pacific Microscopy Conference, Australia
February 5-9, 2012	The International Federation of Societies for Microscopy Bursary Winner in 10 <sup>th</sup> Asia-Pacific Microscopy Conference, Australia